Macroeconomic cycles and bond return predictability*

Stefano Soccorsi[1] Katerina Tsakou[2]

20th April 2025

Abstract

We study the link between the macroeconomy and expected bond returns by dissecting common macroeconomic cycles of different lengths. Two unobservable predictors generate sizeable economic value for investors: an *inflation factor* maximizing macroeconomic cycles of at least 8 years, and a *term spread factor* maximizing cycles of 1 to 3 years. The inflation factor captures the stance of monetary policy as return premia increase when the policy rule becomes "hawkish". The term spread factor reflects investors' perception of business-cycle risk.

JEL subject classification: C38, C53, C55, G11, G12, G17.
Key words: Bond return predictability, frequency-specific factors, band-spectrum principal components, monetary policy, machine learning.

*We are indebted to Sydney Ludvigson, Martin Andreasen and Francesco Bianchi for very useful comments and suggestions on previous versions of this work. We also thank Laura Coroneo, Federico Bandi and participants to various conferences.

[1]s.soccorsi@lancaster.ac.uk — Department of Economics, Lancaster University Management School, UK (corresponding author).

[2]katerina.tsakou@swansea.ac.uk — School of Management, Swansea University, UK.

1. Introduction

According to the expectations hypothesis (EH) of the term structure of interest rates the long-term rate is equal to the average of expected future short rates plus a constant risk premium. While results against the EH span the last four decades (Fama and Bliss, 1987; Campbell and Shiller, 1991; Cochrane and Piazzesi, 2005), the driving forces of time-variation in bond risk premia are still intensely debated. Part of this debate owes to the difficulties in obtaining more accurate out-of-sample excess bond return predictions than the historical average benchmark implied by the EH.

At the same time, however, economic theory provides a clear indication. If investors demand compensation for the risk of recessions as in notable rational expectations models (Campbell and Cochrane, 1999; Wachter, 2006), cyclical variation must be relevant: excess bond returns should be predictable as they evolve with the expected macroeconomic conditions. However, it is not clear what the exact notion of cyclical variation is. Resorting to dynamic factor analysis, Ludvigson and Ng (2009) show that latent common macroeconomic factors contain significant out-of-sample predictive information unspanned by the current yield curve and expected bond returns are consistent with countercyclical risk aversion.[1] More recently, however, Ghysels et al. (2018) find that once real-time data is considered the predictive power of latent macroeconomic factors vanishes.[2]

In this work we consider an alternative approach to the analysis of cyclical variation in real activity which is based on the extraction of cycles of different lengths or, equivalently, decompositions across frequencies. Albeit filtering methods have been used by macroeconomists for the measurement of business cycles, it is just in the last few years that these approaches started to attract considerable interest in finance. Nonetheless, a large body of evidence has already documented frequency-specific effects in asset prices. For example, Dew-Becker and Giglio (2016) show that once the risk of consumption fluctuations in asset pricing models is decomposed in the frequency domain, long-run risk is robustly priced in the equity market. Bandi and Tamoni (2023) study the empirical failure of the classical Consumption CAPM model finding that, unlike consumption growth itself, a 4 to 8 years cyclical component of consumption growth provides a valuable pricing signal and, similarly to the cyclical consumption measured by Atanasov et al. (2020), is a powerful predictor of market returns. Furthermore, Atanasov et al. (2020) show that filtering is theoretically grounded because cyclical consumption closely approximates surplus consumption, the state variable of Campbell and Cochrane (1999)'s external habit formation model.[3]

[1]Similarly, other influential works such as Cooper and Priestley (2009), Greenwood and Vayanos (2014) and Joslin et al. (2014) establish a link between the state of the economy and bond return predictability.

[2]See, however, Caruso and Coroneo (2023) who show that when the latest data vintages available in real time are used, instead of first releases as in Ghysels et al. (2018), predictions of interest rates are nearly as accurate as those obtained with fully revised macroeconomic data.

[3]These are just some of the most notable contributions to a rapidly growing literature. See also Ortu et al. (2013), Kamara et al. (2016), Chaudhuri and Lo (2018), Neuhierl and Varneskov (2021), Bandi et al. (2019), Bandi et al. (2021), Bandi and Su (2023), Huang (2023), Li (2024) among many others.

Inspired by the mounting evidence of frequency-specific effects, we reconsider the predictive power of latent macroeconomic factors along a new dimension: frequency. Are all macroeconomic cycles related to expected bond returns? We propose a new dynamic factor model where common macroeconomic cycles of different lengths are allowed to be driven by different latent factors. Our spectral approach to latent factors turns out to be crucial to reveal the predictive content of real-time macroeconomic data which remains hidden when all frequencies are implicitly aggregated using time-domain techniques. In other words, not all macroeconomic cycles are relevant to expected bond returns.

Determining the length of the common macroeconomic cycles which predict bond returns helps uncover the economic interpretation of our findings. Thanks to this key strength of our approach, we link predictability to the real economy using two frequency-specific factors: the first one is closely related to a component of monetary policy with very persistent effects in the real economy, the second one captures investors' perception of business-cycle risk.

As of today, a burgeoning literature has adopted sophisticated machine learning methods for predicting bond returns. Motivated by the possible existence of irrelevant macroeconomic variation (unrelated to future bond returns) in the predictors and/or nonlinearities of unknown form, increasing interest has been devoted to supervised learning (see Bianchi et al., 2021; Huang et al., 2023; Huang and Shi, 2023, among others). However, when real-time data is used the evidence of predictability in these works comes with at least one of the following two limitations. First, the adoption of overlapping returns which imply an annual holding period. This choice has been criticized since with annual holding periods important short-run dynamics — such as Lehman Brothers' bankruptcy — and business cycle turning points are overlooked (Gargano et al., 2019; Wan et al., 2022). Fan et al. (2022) show that this is far from being an innocuous choice: evidence of predictability in overlapping returns produced by deep learning approaches becomes weak in nonoverlapping returns. Second, there is a difficulty in translating statistical forecasting accuracy into economic value for investors.[4] First raised by Thornton and Valente (2012) and Sarno et al. (2016), this is still an open issue, especially as far as real-time nonoverlapping returns forecasting is concerned. Indeed, to the best of our knowledge, no predictive method considered thus far has been found to generate any economic value in real-time using nonoverlapping excess bond returns. Significant certain equivalent return (CER) gains are found by Eriksen (2017), Bianchi et al. (2021), Huang et al. (2023) using overlapping returns, and by Gargano et al. (2019) using nonoverlapping returns and fully revised macroeconomic data.[5]

While our work follows the recent trend of machine learning methods by allowing for nonlinearity and a high-dimensional space of predictors, our framework is still in the tradition of the seminal work of Ludvigson and Ng (2009) because we consider a dynamic factor model with

[4] For example, in the work of Wan et al. (2022) forecasts which are more accurate in mean square error terms than the historical average benchmark are often associated with poor portfolio performance.

[5] Huang et al. (2023) and the corrigendum to Bianchi et al. (2021) find statistical evidence of predictability based on nonoverlapping returns, but they perform no economic evaluation.

latent common macroeconomic factors. We extend this framework by allowing latent macroeconomic factors to be frequency-specific in the sense that they generate common macroeconomic cycles of given lengths. Our *band spectrum factor model* is nonlinear since in its frequency-domain representation factor loadings are allowed to change across bands of frequencies. At the same time, it has a linear time-domain representation with frequency-specific factors. This allows us to estimate common factors affecting a band of frequencies using a simple generalized principal component estimator obtained by decomposing the covariance matrix by frequencies. So we estimate frequency-specific factors by maximizing specific cyclical comovements of the variables, rather than the comovements associated with common cycles of all lengths as in the standard principal component case. In analogy with Engle (1974) who considers the same setup but with observed factors (band spectrum regressions), we refer to our estimator as *Band Spectrum Principal Components* (BSPCs).

Not all common macroeconomic factors predict bond returns. In fact, Ludvigson and Ng (2009) show that it is necessary to disentangle relevant from irrelevant macroeconomic factors, and identify a subset of factors with predictive power via an extensive model selection procedure based on the minimization of a BIC criterion. Similarly to Huang et al. (2023), we do so by adopting a supervised learning approach based on the principle of statistical sufficiency: rather than searching for a subset of factors which predicts bond returns, we focus on the space they span. This space, referred to as *central subspace*, is identified by projecting each predictor onto observable proxies before extracting principal components (Fan et al., 2017, 2021). Similarly to identification methods via instrumental variables, these proxies fulfill exogeneity since they are orthogonal to common macroeconomic factors unrelated to future bond returns.[6] Our procedure is the same but we extract BSPCs. That is, our predictors are factors extracted by choosing proxies for the central subspace and a band of frequencies. In so doing, we are able to study whether excess bond returns live in a subspace of factors generating common macroeconomic cycles of given lengths.

From a real-time macroeconomic dataset of 54 variables, we extract two frequency-specific factors across different bands of frequencies, one using inflation as a proxy, the other the term spread. This is in accordance with a broad literature combining yield factors and possibly unspanned macroeconomic factors. For example, Cieslak and Povala (2015) adopt a decomposition based on a trend-inflation factor and cyclical components of yields.

While weak or no evidence of predictability is found when full-spectrum predictors are considered, the picture is remarkably different when we instead focus on specific bands of frequencies. Two powerful predictors are obtained within two different spectral bands: the one by taking factors driving macroeconomic cycles of at least 8 years related to the inflation, the other macroeconomic cycles of 1 to 3 years related to the term spread. Hereafter we refer to them as *inflation factor* and *term spread factor*, respectively. Being related with inflation targeting,

[6] See also Kelly et al. (2019) for a similar method for the cross-section of returns based on unobserved factors with loadings related to observable instruments.

the inflation factor is relatively more accurate at the short end of the yield curve, whereas the term spread factor is relatively more accurate for longer maturities which are more exposed to variation in the risk premium. Using these two predictors, we find evidence of predictability in both statistical and economic terms for investors of various kinds (i.e. with mean-variance or power utility and a range of risk aversions). To the best of our knowledge, the finding of significant CER gains using real-time data and nonoverlapping returns is novel in this literature.

The economic picture arising from our predictive exercise closely ties bond return predictability with monetary policy. First, the inflation factor, which is found to be unspanned by the usual yield curve factors (level, slope and curvature) or forward rates (Cochrane and Piazzesi (2005)'s factor), predicts survey inflation expectations. Second, it replicates the dynamics of risk premia generated by the switches in the stance of monetary policy studied by Bianchi et al. (2022): according to their work, risk premia increase when the Federal Reserve changes the monetary policy rule to respond more vigorously to inflation by pushing the federal fund rate above the natural rate, and so enlarging a *monetary policy spread* (the gap between the real federal fund rate and the natural rate). In fact, the predictive power of our inflation factor is found only during the hawkish monetary policy regimes identified by Bianchi et al. (2022), and the inflation factor significantly predicts the turning points of the monetary policy spread. Consistent with the fact that the inflation factor maximizes cycles of at least 8 years in length, the shifts in the monetary policy rule considered by Bianchi et al. (2022) have long-lasting effect on real variables.

Our term spread factor maximizing cycles of 1 to 3 years in length seems to confirm the findings of Fama and French (1989) who conclude that the "term spread is more closely related to the *shorter-term* business cycles identified by NBER", and resembles the *cycle factor* identified by Cieslak and Povala (2015), that is, a component of yields which is orthogonal to a slow-moving average of inflation and whose predictive power increases across maturities. In line with a business-cycle risk interpretation, our term spread factor predicts recessions, and is a hedge against the risk of recessions as investors do not demand a compensation for exposure to it when the economy is contracting. This evidence could also be related to monetary policy. Andreasen et al. (2021), who analyse in depth the role of the term spread along the phases of business cycles, similarly to us find a dual role of the slope of the yield curve (hedge in recession, risk factor in expansion), and conclude that this is a sign that during recessions investors expect the Federal Reserve to cut rates and close the output gap.

Finally, we reaffirm three main conclusions of Ludvigson and Ng (2009). First, we confirm the existence of comovements between the macroeconomy and predictable variation in excess bond returns which are captured by some subset of latent macroeconomic factors. Second, we reject the expectations hypothesis in favour of countercyclical risk aversion. Third, we add to the evidence against the "spanning hypothesis" and suggests that affine term structure models should include macroeconomic information which is not spanned by the current yield curve.[7]

[7] Among others, see Chernov and Mueller (2012), Joslin et al. (2014), Coroneo et al. (2016) who also associate

The rest of this paper is as follows. In Section 2 we outline all the methodological aspects of our work: our band spectrum factor model, its estimation, and the supervised learning method we adopt to obtain predictors for excess bond returns. Section 3 is dedicated to the yield data and the real-time macroeconomic dataset used to construct our predictors. Out-of-sample forecasting results are presented in Section 4. In Section 5 we open the black box of our factors and so establish the links between predictability and the real economy. Section 6 concludes.

2. Methodology

There are two difficulties associated with the widespread use of principal components in predictive regressions for bond returns (typically common factors estimated using large macroeconomic datasets).

First, being linear combinations with maximum variance, principal components account for variables' comovements at all frequencies by aggregating cycles of all lengths. Albeit this is adequate for predicting processes of various kinds, mounting evidence that risk varies across frequencies motivates us to investigate whether macroeconomic cycles of different lengths have the same relationship, or any relationship whatsoever, with bond returns. If some macroeconomic cycles contain no predictive power for excess bond returns, the exclusion of the corresponding frequencies reduces the measurement error in the predictors. This means that accurate predictors cannot be obtained aggregating cycles of all lengths. Similarly, if cycles of different lengths do not have the same relationship with bond returns, frequency-specific predictive systems should be allowed for. In these cases, principal components become suboptimal predictors.

In order to shed light on the possible existence of frequency-specific predictors, we develop an approach to account for comovements among cycles of given lengths. In Section 2.1, we introduce a novel factor model with frequency-specific factors. The model arises as a natural consequence of variation in the factor loadings across spectral bands, which we allow for following the seminal work of Engle (1974) on band-spectrum regressions. In Section 2.2, we propose an estimator for frequency-specific factors. Our *band spectrum principal components* are linear combinations of variables with maximum variance only within a band of frequencies, hence they generalize principal components.

Second, not all macroeconomic comovements need to contain information on future bond returns. In fact, Ludvigson and Ng (2009) found that only a subset of common macroeconomic factors predict bond returns. In Section 2.3 we combine band spectrum principal components with supervised learning so that we allow our predictors to live in a subspace of frequency-specific common factors. In so doing, our predictors are not contaminated by common macroeconomic cycles unrelated to predictable variation in excess bond returns.

unspanned macroeconomic factors with inflation.

2.1. Frequency-specific factors

Consider a $T \times N$ panel $\mathbf{X} \coloneqq \{x_{it};\ i = 1, \dots, N;\ t = 1, \dots, T\}$ of mean-zero weakly stationary variables with a latent factor structure

$$\mathbf{X}_t = \Lambda \mathbf{F}_t + \mathbf{e}_t \tag{1}$$

where $\mathbf{X}_t$ is the N-dimensional vector $(x_{1t}, x_{2t}, \dots, x_{Nt})'$, Λ a $N \times r$ matrix of loadings, $\mathbf{F}_t$ an r-dimensional vector of unobservable factors, $\mathbf{e}_t$ a N-dimensional vector of idiosyncratic terms which are weakly cross-correlated in the sense of Chamberlain and Rothschild (1983) and Connor and Korajczyk (1986), and orthogonal to $\mathbf{F}_t$ at all leads and lags.[8] Being the factors common to all cross-sectional units $x_{1t}, \cdots, x_{Nt}$, the term $\Lambda \mathbf{F}_t$ is known as the common component of $\mathbf{X}_t$ and interpreted as the effect of comovements between the variables. In this work we focus on a frequency-specific analysis of those comovements. Letting $\iota = \sqrt{-1}$ be the imaginary unit, ω some frequency in $[-\pi, \pi]$, we have the Fourier transforms $\mathcal{X}_\omega = T^{-1/2} \sum_{t=1}^{T} \mathbf{X}_t e^{-\iota\omega t}$, $\mathcal{F}_\omega = T^{-1/2} \sum_{t=1}^{T} \mathbf{F}_t e^{-\iota\omega t}$, $\mathcal{E}_\omega = T^{-1/2} \sum_{t=1}^{T} \mathbf{e}_t e^{-\iota\omega t}$. The factor model (1) allows for a frequency-domain representation

$$\mathcal{X}_\omega = \Lambda \mathcal{F}_\omega + \mathcal{E}_\omega$$

which shows that the relationship between the cycles of length $2\pi/\omega$ of $\mathbf{X}_t$ and those of the same length of the common factors $\mathbf{F}_t$ is constant and independent of ω.

We are interested in a more general framework in which comovements are allowed to vary across frequencies. Consider, for example, a partition of $[-\pi, \pi]$ into two disjoint subsets Ω_1 and Ω_2.[9] Allowing for different cyclical comovements across these two bands of frequencies calls for a frequency-domain representation

$$\mathcal{X}_\omega = \begin{cases} \Lambda_1 \mathcal{F}_\omega + \mathcal{E}_\omega & \omega \in \Omega_1 \\ \Lambda_2 \mathcal{F}_\omega + \mathcal{E}_\omega & \omega \in \Omega_2 \end{cases} \tag{2}$$

where, similarly to Engle (1974), coefficients (factor loadings) are allowed to vary across frequencies. Equation (2) can be rewritten as

$$\mathcal{X}_\omega = \Lambda_1 \mathcal{F}_{\omega,1} + \Lambda_2 \mathcal{F}_{\omega,2} + \mathcal{E}_\omega \tag{3}$$

[8] Following Chamberlain and Rothschild (1983) and Connor and Korajczyk (1986), we consider an approximate factor structure for which the cross-correlation generated by the idiosyncratic components is asymptotically negligible. Orthogonality at all leads and lags between the factors and idiosyncratic terms is stronger than the weak dependence as in Assumption D of Bai and Ng (2002), but needed for the estimation of the spectral density matrix as in the strand of literature on generalized dynamic factor models initiated by Forni et al. (2000).

[9] For simplicity and without loss of generality, two bands of frequencies are considered in this section. In the empirical part of this work we consider four bands.

where $$\mathcal{F}_{\omega,1}=\begin{cases}\mathcal{F}_\omega & \omega\in\Omega_1\\ \mathbf{0} & \omega\in\Omega_2\end{cases}\qquad\text{and}\qquad \mathcal{F}_{\omega,2}=\begin{cases}\mathbf{0} & \omega\in\Omega_1\\ \mathcal{F}_\omega & \omega\in\Omega_2\end{cases}$$

As a result, we are interested in the *band spectrum factor model*

$$\mathbf{X}_t=\Lambda_1\mathbf{F}_t\left(\Omega_1\right)+\Lambda_2\mathbf{F}_t\left(\Omega_2\right)+\mathbf{e}_t \tag{4}$$

where $\mathbf{F}_t\left(\Omega_1\right)$, $\mathbf{F}_t\left(\Omega_2\right)$, defined as the inverse Fourier transforms of $\mathcal{F}_{\omega,1}$ and $\mathcal{F}_{\omega,2}$, are common factors across the spectral components of $\mathbf{X}_t$ at frequencies ω in Ω_1 and Ω_2, respectively.[10] Being the factors $\mathbf{F}_t\left(\Omega\right)$ unrelated to any frequency out of the band Ω, we refer to them as frequency-specific factors which generate the common cycles of $\mathbf{X}_t$ of length $2\pi/\omega$ for all frequencies $\omega\in\Omega$. So, to the nonlinear frequency-domain representation (2) corresponds a factor model (4) which is linear in the frequency-specific factors.

The band spectrum factor model (4) implies a canonical decomposition of the covariance matrix

$$\mathbf{C}_0\equiv E\left(\mathbf{X}_t\mathbf{X}_t'\right)=\Lambda_1E\left(\mathbf{F}_t\left(\Omega_1\right)\mathbf{F}_t\left(\Omega_1\right)'\right)\Lambda_1'+\Lambda_2E\left(\mathbf{F}_t\left(\Omega_2\right)\mathbf{F}_t\left(\Omega_2\right)'\right)\Lambda_2'+E\left(\mathbf{e}_t\mathbf{e}_t'\right) \tag{5}$$

for which the first term is the covariance of the comovements at frequencies in Ω_1, the second is the covariance of the comovements at frequencies in Ω_2, and the last one is the "weak" (i.e. asymptotically negligible) covariance generated by idiosyncratic cycles of all lengths.[11]

In order to estimate the frequency-specific factors $\mathbf{F}_t\left(\Omega\right)$, one needs to disentangle common from idiosyncratic covariances in Ω. Of course, this is only possible with a prior estimate of the overall (common and idiosyncratic) comovements in Ω. Exploiting the inverse Fourier transform $\mathbf{C}_0=\int_{-\pi}^{\pi}\mathbf{S}\left(\omega\right)\ d\omega$, where $\mathbf{S}\left(\omega\right)=\left(2\pi\right)^{-1}\sum_{k=-\infty}^{\infty}e^{-\imath k\omega}\mathbf{C}_k$ is the spectral density matrix at frequency ω and $\mathbf{C}_k=E\left(\mathbf{X}_t\mathbf{X}_{t-k}'\right)$, the component of $\mathbf{C}_0$ due to the covariance among all common and idiosyncratic cycles in Ω is

$$\mathbf{C}_0\left(\Omega\right)\coloneqq\int_{\omega\in\Omega}E\left(\mathcal{X}_\omega\mathcal{X}_\omega'\right)d\omega=\int_{\omega\in\Omega}\mathbf{S}\left(\omega\right)d\omega \tag{6}$$

In the rest of this paper we refer to $\mathbf{C}_0\left(\Omega\right)$ as the *band spectrum covariance* matrix of $\mathbf{X}_t$ in Ω.

[10]The derivation of $\mathbf{F}_t\left(\Omega\right)$ corresponds to the frequency-domain band-pass filter (Priestley, 1981, p. 274–275). Albeit not as popular as its approximate time-domain counterpart, also this method has been applied to the to the measurement of business cycles (see Englund et al., 1992; Hassler et al., 1994).

[11]To see this, it is enough to note that

$$\begin{aligned}\mathbf{C}_0=\int_{-\pi}^{\pi}E\left(\mathcal{X}_\omega\mathcal{X}_\omega'\right)\ d\omega&=\Lambda_1\int_{-\pi}^{\pi}E\left(\mathcal{F}_{\omega,1}\mathcal{F}_{\omega,1}'\right)\ d\omega\ \Lambda_1'\ +\ \Lambda_2\int_{-\pi}^{\pi}E\left(\mathcal{F}_{\omega,2}\mathcal{F}_{\omega,2}'\right)\ d\omega\ \Lambda_2'\ +E\left(\mathbf{e}_t\mathbf{e}_t'\right)\\&=\Lambda_1\int_{\omega\in\Omega_1}E\left(\mathcal{F}_\omega\mathcal{F}_\omega'\right)\ d\omega\ \Lambda_1'\ +\ \Lambda_2\int_{\omega\in\Omega_2}E\left(\mathcal{F}_\omega\mathcal{F}_\omega'\right)\ d\omega\ \Lambda_2'\ +E\left(\mathbf{e}_t\mathbf{e}_t'\right)\end{aligned}$$

since, $\int_{\omega\in\Omega_2}E\left(\mathcal{F}_{\omega,1}\mathcal{F}_{\omega,1}'\right)\ d\omega=\mathbf{0}$, $\int_{\omega\in\Omega_1}E\left(\mathcal{F}_{\omega,2}\mathcal{F}_{\omega,2}'\right)\ d\omega=\mathbf{0}$, and $\mathbf{e}_t$ is orthogonal to all common factors.

2.2. Band Spectrum Principal components

The estimation of common factors via asymptotic principal components is widespread and well-known (Bai and Ng, 2002; Stock and Watson, 2002a; Forni et al., 2000). Assuming that $T^{-1}\sum_{t=1}^{T}\mathbf{F}_t\mathbf{F}_t'$ and $N^{-1}\Lambda\Lambda'$ converge to some positive definite matrices (with distinct eigenvalues) as T and N grow to infinity is enough to ensure that r eigenvalues of $\Lambda T^{-1}\sum_{t=1}^{T}\mathbf{F}_t\mathbf{F}_t'\Lambda'$ diverge as N grows to infinity. This implies that r eigenvalues of the covariance matrix of the data $\mathbf{C}_0$ diverge as well. Further assuming that the covariance matrix of the idiosyncratic terms has bounded eigenvalues as N grows to infinity, and some moment conditions, the space spanned by the factors can be estimated from the eigenvalue-eigenvector decomposition of the sample covariance matrix of the data.

The covariance structure (5) generated by the band spectrum factor model (4) suggests that frequency-specific factors $\mathbf{F}_t(\Omega_1)$ and $\mathbf{F}_t(\Omega_2)$ can be estimated following the same logic within a band of frequencies. Consider the covariance in the band Ω_1

$$\begin{aligned}\mathbf{C}_0(\Omega_1) &= \int_{\omega\in\Omega_1} E\left(\mathcal{X}_\omega\mathcal{X}_\omega'\right) = \Lambda_1\int_{\omega\in\Omega_1} E\left(\mathcal{F}_{\omega,1}\mathcal{F}_{\omega,1}'\right)\, d\omega\ \Lambda_1' + \int_{\omega\in\Omega_1} E\left(\mathcal{E}_\omega\mathcal{E}_\omega'\right)\, d\omega \\ &= \Lambda_1 E\left(\mathbf{F}_t(\Omega_1)\mathbf{F}_t(\Omega_1)'\right)\Lambda_1' + \int_{\omega\in\Omega_1} E\left(\mathcal{E}_\omega\mathcal{E}_\omega'\right)\, d\omega \end{aligned} \tag{7}$$

where we used equation (3) and (4). Assuming that $N^{-1}\Lambda_1\Lambda_1'$ and $T^{-1}\sum_{t=1}^{T}\mathbf{F}_t(\Omega_1)\mathbf{F}_t(\Omega_1)'$ converge to positive definite matrices (with distinct eigenvalues) as $N\to\infty$ and $T\to\infty$ respectively, we have that r eigenvalues of $\mathbf{C}_0(\Omega_1)$ diverge asymptotically. This, combined with the usual assumptions on the idiosyncratic errors mentioned above, implies that as N, T jointly grow to infinity, the second term of (7) becomes negligible and the eigenvectors associated with largest r eigenvalues of $\mathbf{C}_0(\Omega_1)$ span the space of $\mathbf{F}_t(\Omega_1)$. This motivates the *band spectrum principal component* estimator

$$\hat{\mathbf{F}}_t(\Omega_1) = \sqrt{T}V_r'(\Omega_1)\mathbf{X}_t \tag{8}$$

where $V_r(\Omega_1) = (v_1(\Omega_1), v_2(\Omega_1), \ldots\ v_r(\Omega_1))$ and $v_j(\Omega_1)$ is the eigenvector associated with the j-th largest eigenvalue of $\hat{\mathbf{C}}_0(\Omega_1)$ for $j\le r$. Similarly, $\hat{\mathbf{F}}_t(\Omega_2) = \sqrt{T}V_r'(\Omega_2)\mathbf{X}_t$.

The band spectrum covariance $\mathbf{C}_0(\Omega)$ can be estimated by replacing $\mathbf{S}(\omega)$ in equation (6) with its estimate. We use the lag-window estimator

$$\hat{\mathbf{S}}(\omega) = \frac{1}{2\pi}\sum_{j=-M_T}^{M_T} K_j(M_T)\, e^{-\iota j\omega}\hat{\mathbf{C}}_j \tag{9}$$

where $\hat{\mathbf{C}}_j$ is the sample estimate of $\mathbf{C}_j$, and $K_j(M_T) = 1-\frac{|j|}{M_T}$ is the triangular kernel with bandwidth M_T, which is known to be consistent if $T^{-1}M_T\to 0$ as $T\to\infty$ and $M_T\to\infty$. In practice $M_T = \lfloor\sqrt{T}\rfloor$ is often chosen, where $\lfloor\cdot\rfloor$ denotes the floor function. In the rest of this paper we refer to such estimator as

$$\hat{\mathbf{C}}_0(\Omega) = \sum_{\omega_k \in \Omega} \hat{\mathbf{S}}(\omega_k) \; d\omega \approx \int_{\omega \in \Omega} \hat{\mathbf{S}}(\omega) \; d\omega \tag{10}$$

where $\omega_k = \pi k/T$ with $k = -T, -T+1, \cdots, T$ is the generic Fourier frequency.

In Appendix A we show that the BSPCs consistently estimate the space spanned by frequency-specific factors and provide simulation evidence that the estimator performs well in finite samples.

2.2.1. Discussion

There are important antecedents to our band spectrum principal component estimator. The idea of estimating models on a band of frequencies dates back to the regression analysis with distributed lags of Hannan (1963, 1965). The most direct antecedent is however the seminal work on band spectrum regressions of Engle (1974) who, interested in studying whether slope coefficients change across frequencies, considers a usual least squares framework limited to a band of frequencies. Although ours is a high-dimensional problem with a set of predictors driven by unobserved factors, our band spectrum principal component estimator is closely related to band spectrum regressions since it minimizes the least square objective function $\int_{\omega \in \Omega} (\mathcal{X}_\omega - \Lambda \mathcal{F}_\omega)' (\mathcal{X}_\omega - \Lambda \mathcal{F}_\omega) \; d\omega$. Indeed, this problem reverts to:

- OLS when $\Omega = [-\pi, \pi]$ and $\mathbf{F}_t$ is observed;
- principal components when $\Omega = [-\pi, \pi]$ and $\mathbf{F}_t$ is unobserved;
- Engle's band spectrum regressions when Ω is a subset of $[-\pi, \pi]$ and $\mathbf{F}_t$ is observed.

Our band spectrum principal component problem corresponds to the case in which Ω is a subset of $[-\pi, \pi]$ and $\mathbf{F}_t$ is unobserved.

Being the goal of band spectrum analysis the detection of possible frequency-specific effects, an essential property of these estimators is that when no frequency-specific effect holds the estimators yield inefficient estimates as compared to their full spectrum counterparts. For example, if the data generating process is a standard linear regression model band spectrum regressions across different bands yield inefficient estimates of the same slope coefficients which are constant across frequencies. Our BSPC estimator obeys the corresponding property when the loadings do not vary across bands. Returning to the band spectrum model (4), the BSPC estimator is such that $\hat{\mathbf{F}}(\Omega_j) = \mathbf{X}\hat{\Lambda}_j \left(\hat{\Lambda}_j \hat{\Lambda}_j'\right)^{-1}$, so the same estimate across the two bands is obtained when $\Lambda_1 = \Lambda_2$ and loadings are consistently estimated. Intuitively, the BSPC becomes a relatively inefficient but consistent estimator of $\mathbf{F}$ since it only uses a band of frequencies even if there is no such thing as frequency-specific factor that can be obtained from the frequency-domain representation (2) when loadings are constant over the spectrum.

Note that even in absence of frequency-specific factors $\mathbf{F}(\Omega_j)$ remains well-defined as it corresponds to the band-pass filtered version of $\mathbf{F}$ in Ω_j. For this reason, in the simulation exercises of Appendix A we measure both the distance between $\hat{\mathbf{F}}(\Omega_j)$ and $\mathbf{F}(\Omega_j)$ (which vanishes asymptotically under frequency-specific effects) and that between $\hat{\mathbf{F}}(\Omega_j)$ and $\mathbf{F}$ (which vanishes asymptotically under no frequency-specific effects).

Accounting for the use of spectral regressions and closely related methods for the analysis of frequency-specific effects in economics and finance goes beyond the scope of this paper. We refer to the recent survey of Bandi and Tamoni (2022) for an up-to-date, comprehensive discussion of this vast strand of literature.

2.3. Forecasting bond returns: supervised learning and band spectrum principal components

The use of principal component analysis in economics and finance is widespread because generally the space spanned by a high-dimensional process $\mathbf{X}_t = (x_{1t}, x_{2t}, \cdots, x_{Nt})$, such as a collection of macroeconomic variables, is well approximated by that spanned by a small number of principal components $\left(\hat{F}_{1t}, \hat{F}_{2t}, \cdots, \hat{F}_{rt}\right)$, with $r \ll N$. Indeed, principal components are widely used to estimate unobservable common factors (Bai and Ng, 2002; Forni et al., 2000; Stock and Watson, 2002a) and predict macroeconomic aggregates (see Stock and Watson, 2002b; Giannone et al., 2008; Forni et al., 2018, among many others).

Predicting a specific target, such as excess bond returns, is a different problem than fitting a collection of macroeconomic variables or aggregates. Even if the macroeconomy contains predictive information for bond returns, some common macroeconomic factors may represent macroeconomic fluctuations unrelated to bond returns. In this case, it becomes necessary to identify a subspace the predictive signal lives in which is spanned by a subset of common factors. For example, Ludvigson and Ng (2009) perform a model selection procedure for which 8 principal components and powers thereof are considered in the minimisation of a BIC criterion. Their selected specification is based on a linear combination of $\left(\hat{F}_{1t}, \hat{F}_{1t}^3, \hat{F}_{3t}, \hat{F}_{4t}, \hat{F}_{8t}\right)$.

The problem of estimating a predictive signal living in a common factor subspace has been widely considered in the statistical learning literature. Supervised statistical learning solves this problem in a simpler manner by embedding the individual predictive power of each covariate x_{1t}, x_{2t}, $\ldots$, x_{Nt} into the extraction of the predictive signal via principal components. Using correlation as a measure of predictive power, Bair et al. (2006) estimate predictors as principal components of a subset of covariates that correlate well with the predictive target.[12] Another strand of this literature is based on the idea of sufficiency for estimating a minimal common factor subspace, which is referred to as the *central subspace* (Cook, 2007). This subspace is minimal because, despite dimension reduction, it contains all the information in the covariates for the predictive target.[13] These methods are based on the projection of each covariate x_{it} onto

[12]Subsequent works based on this approach include Bai and Ng (2008) and Giglio et al. (2023).

[13]That is, the conditional distribution of the target given the predictors $\mathbf{X}$ is the same as that given a lower-

proxies for the central subspace, such as the observed past of the predictive target (Cook and Forzani, 2008; Huang et al., 2022, 2023) and/or other observed variables (Fan et al., 2017, 2021). Principal components are then applied to the projected (or fitted) values of the covariates.

In a linear predictive model the dimension of the central subspace is one.[14] For example, in the model $rx_{t+1} = \mu + \lambda_{rx}' \mathbf{F}_t + \varepsilon_{t+1}$ (where λ_{rx} may have one or more zero elements), the central subspace is Span $(\lambda_{rx}' \mathbf{F}_t)$ and $\lambda_{rx}' \mathbf{F}_t$ is a single sufficient index. If, also, $\mathbf{F}_t$ obeys a standard factor model (1), one principal component of projected data is sufficient. This is so because, if $\mathbf{z}_t$ is a vector of proxies for the central subspace, each projection $\hat{x}_{it}(\mathbf{z}) = \text{Proj}(x_{it}|\mathbf{z}_t)$ of x_{it} onto $\mathbf{z}_t$ has a common component which is proportional to $\lambda_{rx}' \mathbf{F}_t$ and an idiosyncratic term orthogonal to it which does not survive cross-sectional aggregation. Therefore, the first principal component of $\hat{x}_{1t}(\mathbf{z})$, $\hat{x}_{2t}(\mathbf{z}), \cdots, \hat{x}_{Nt}(\mathbf{z})$ estimates the sufficient single factor $\lambda_{rx}' \mathbf{F}_t$.

In this work we investigate whether the central subspace for excess bond returns is spanned by frequency-specific factors. Consider, for example, $rx_{t+1} = \mu + \lambda_{rx}' \mathbf{F}_t(\Omega) + \varepsilon_{t+1}$. In this scenario, the central subspace becomes Span $(\lambda_{rx}' \mathbf{F}_t(\Omega))$ and the sufficient single factor $\lambda_{rx}' \mathbf{F}_t(\Omega)$ is estimated by a band spectrum principal component at the band Ω of $\hat{x}_{1t}(\mathbf{z})$, $\hat{x}_{2t}(\mathbf{z}), \cdots,$ $\hat{x}_{Nt}(\mathbf{z})$. This example can be extended by allowing for frequency-specific factors in different bands, such as $rx_{t+1} = \mu + \lambda_{rx,1}' \mathbf{F}_t(\Omega_1) + \lambda_{rx,2}' \mathbf{F}_t(\Omega_2) + \varepsilon_{t+1}$. In this case, allowing for $\lambda_{rx,1}' \mathbf{F}_t(\Omega_1)$ to be proxied by $\mathbf{z}_t^{(1)}$ and $\lambda_{rx,2}' \mathbf{F}_t(\Omega_2)$ by $\mathbf{z}_t^{(2)}$, for the central subspace we need one band spectrum principal component in Ω_1 of projected data $\hat{x}_{1t}\left(\mathbf{z}^{(1)}\right)$, $\hat{x}_{2t}\left(\mathbf{z}^{(1)}\right), \cdots, \hat{x}_{Nt}\left(\mathbf{z}^{(1)}\right)$, and one in Ω_2 of $\hat{x}_{1t}\left(\mathbf{z}^{(2)}\right)$, $\hat{x}_{2t}\left(\mathbf{z}^{(2)}\right), \cdots, \hat{x}_{Nt}\left(\mathbf{z}^{(2)}\right)$.

In full generality, our predictors are obtained as follows. Letting $\mathbf{z}_t$ now be a vector of proxies for the central subspace at frequencies in Ω, we take the projected values $\hat{x}_{it}(\mathbf{z})$ where $\hat{x}_{it}(\mathbf{z})$ is an estimate of the component of x_{it} driven by the subset of Ω-specific factors that predicts excess bond returns. Letting $\hat{\mathbf{C}}_{\hat{x},0}(\Omega, \mathbf{z})$ be the band spectrum covariance matrix of the $T \times N$ panel of projected data $\hat{\mathbf{X}}(\mathbf{z}) := \{\hat{x}_{it}(\mathbf{z});\ i = 1, \ldots, N;\ t = 1, \ldots, T\}$, we consider band spectrum principal components of projected data

$$
\begin{aligned}
v_{\hat{x}}^*(\Omega, \mathbf{z}) &= \underset{v \in \mathbb{R}^N,\ v'v=1}{\arg\max}\ v' \hat{\mathbf{C}}_{\hat{x},0}(\Omega, \mathbf{z})\, v \\
\hat{F}_t(\Omega, \mathbf{z}) &= v_{\hat{x}}^*(\Omega, \mathbf{z})' \hat{\mathbf{X}}_t(\mathbf{z})
\end{aligned}
\tag{11}
$$

where $\hat{\mathbf{X}}_t(\mathbf{z}) = (\hat{x}_{1t}(\mathbf{z}), \hat{x}_{2t}(\mathbf{z}), \cdots, \hat{x}_{Nt}(\mathbf{z}))'$. As discussed in Section 2.2, for the band spectrum covariance we use the plugin estimator

$$
\hat{\mathbf{C}}_{\hat{x},0}(\Omega, \mathbf{z}) = \sum_{\omega_k \in \Omega} \hat{\mathbf{S}}_{\hat{x}}(\omega_k)\ d\omega \tag{12}
$$

where $\hat{\mathbf{S}}_{\hat{x}}(\omega)$ is the estimated spectral density matrix of $\hat{\mathbf{X}}(\mathbf{z})$ obtained using a lag-window

dimensional transformation of $\mathbf{X}$.

[14] The dimension of the central subspace is greater than one in the nonlinear case considered by Fan et al. (2017).

estimator as in equation (9).

Algorithm: Projected Band Spectrum Principal Components

1. For $i = 1, \cdots, N$, take the projections $\hat{x}_{it}(\mathbf{z}) = \text{Proj}(x_{it}|\mathbf{z}_t)$.
2. Estimate the spectral density $\mathbf{S}_{\hat{x}}(\omega)$ of $\hat{\mathbf{X}}(\mathbf{z})$ using a lag-window estimator (9).
3. Estimate the band-spectrum covariance matrix $\mathbf{C}_{\hat{x},0}(\Omega, \mathbf{z})$ as in equation (12).
4. Obtain $\hat{F}_t(\Omega, \mathbf{z})$ as in equation (11).

In the empirical part of this work, we predict one month ahead excess bond returns using the predictors $\hat{F}_t(\Omega, \mathbf{z})$ for different choices of Ω and $\mathbf{z}$.

Allowing for frequency-specific factors is the main element of novelty with respect to other existing supervised learning methods based on a large number of predictors with a common factor structure, projections onto observed proxies, and principal component estimators. The closest approach to ours is that of Huang et al. (2022) which is also based on a linear forecasting equation. Fan et al. (2017) allow the predictive target to be some unknown nonlinear function of its sufficient predictive indices (whose dimension exceeds one because of nonlinearity), while Fan et al. (2021) also consider robust estimation based on Huber loss minimization. In both works observed covariates are exploited using a projected principal component estimator (Fan et al., 2016). Huang et al. (2023) further extend Fan et al. (2017) in order to allow for weak factors.

3. Data

3.1. Excess bond returns

The (continuously compounded) yield of a n-year bond is

$$y_t^{(n)} = -\frac{1}{n} p_t^{(n)}$$

where $p_t^{(n)} = \ln P_t^{(n)}$, and $P_t^{(n)}$ denotes the time t nominal price of a bond with n-years left to maturity. The excess return of a risky n-year bond is given by the difference between the log return from a n-year bond bought at time t and sold m months later, and the yield on a m-period risk-free rate at time t.

$$rx_{t+m}^{(n)} = p_{t+m}^{\left(n-\frac{m}{12}\right)} - p_t^{(n)} - \frac{m}{12} y_t^{\left(\frac{m}{12}\right)} = n y_t^{(n)} - \left(n - \frac{m}{12}\right) y_{t+m}^{\left(n-\frac{m}{12}\right)} - \frac{m}{12} y_t^{\left(\frac{m}{12}\right)} \tag{13}$$

where m is the holding period and $y_t^{\left(\frac{m}{12}\right)}$ is the annualized m-period risk-free rate.

Setting $m = 1$, we construct (monthly) nonoverlapping excess bond returns. In so doing, we follow recent works (such as Gargano et al., 2019; Wan et al., 2022; Borup et al., 2023) which advocate the use of nonoverlapping returns versus the commonly used monthly overlapping returns corresponding to an annual holding period ($m = 12$). Generally, there are a number of reasons for doing so. First, there are important short-lived dynamics in excess bond returns, such as Lehman Brothers' bankruptcy, which cannot be captured with annual holding periods. Second, overlapping returns present difficulties with the turning points of business cycles, which bear an intimate relationship with return predictability. Third, nonoverlapping returns are free from the serial correlation in residuals introduced by overlapping observations which exacerbate the inferential problems described by Bauer and Hamilton (2018).[15] More specifically, in this work we are interested in characterising the predictability of bond returns related to macroeconomic cycles of different lengths: adopting overlapping returns would impair the analysis of cycles shorter than 1 year.

Yield data is taken from the zero-coupon Treasury yield curve dataset of Liu and Wu (2021) considering maturities up to 10 years. This is the same choice as in works conducting a similar out-of-sample predictive exercise, such as Bianchi et al. (2021), Fan et al. (2022). This dataset is obtained using a nonparametric kernel-smoothing method which compares favourably to the popular alternative dataset of Gürkaynak et al. (2007) as it takes into account Treasury bills and securities with less than 3 months to maturity and is found to contain smaller pricing errors.[16]

3.2. Real-time macroeconomic data

We obtain real-time macroeconomic data from the ALFRED database published by the Federal Reserve Bank of St. Louis. Apart from minor differences due to discontinued variables, our dataset is similar to that adopted by Ghysels et al. (2018) and Wan et al. (2022).[17] We observe $N = 54$ variables which can be broadly classified as "output and income", "labor market", "housing", "money and credit", "prices". Most of these variables are nonstationary and need being transformed to achieve stationarity. After these transformations, reported in Appendix B, the sample observations available span from August 1972 until December 2020. Some variables are available at earlier dates, however this is the largest sample available without missing values.

We observe a total of 465 vintages running from April 1982 to December 2020.[18] With no ragged-edge data, our first vintage dated April 1982 would be based on 117 data points from August 1972 onwards. However, these variables are available with a publication delay, typically one or two months. For example, our April 1982 vintage contains variables observed from August 1972 until to March 1982 and some from August 1972 until to February 1982. For each vintage we cope with this problem by discarding the first few observations of the variables with a shorter publication delay until a balanced panel is obtained. This leaves us, for example,

[15] Gargano et al. (2019) find that, indeed, these problems largely disappear with nonoverlapping returns.

[16] The popular dataset of Fama and Bliss (1987) is instead unfit to our analysis since it starts from the 1-year maturity, hence it cannot be used to construct nonoverlapping returns.

[17] More precisely, 8 out of 60 variables used in Ghysels et al. (2018) were discontinued in December 2015 and, thus, we exclude them. Our dataset includes the remaining 52 variables plus *CURRDD* and *DEDEPSL* also used by Wan et al. (2022).

[18] Infrequently, two vintages of a variable are released in a month. In such cases we take the last vintage of the month. If no vintage is published in a month we take the last vintage of the previous month.

with an April 1982 vintage of our full dataset collecting all variables with an actual sample size of 115 observations.

Finally, we remove outliers without looking into the future and standardize the data before the estimation of our predictors.[19]

As a preliminary investigation into our macroeconomic dataset, we use the full sample in our latest vintage dated December 2020 of dimension $(T, N) = (579, 54)$ to decompose the covariance matrix into its components in the frequency bands indicated below.

$\mathit{\Omega}_1 = [2\pi/12, \pi]$ corresponding to cycles of length up to 1 year;

$\mathit{\Omega}_2 = [2\pi/36, 2\pi/12]$ corresponding to cycles of length between 1 and 3 years;

$\mathit{\Omega}_3 = [2\pi/96, 2\pi/36]$ corresponding to cycles of length between 3 and 8 years;

$\mathit{\Omega}_4 = [0, 2\pi/96]$ corresponding to cycles of length of 8+ years,

where, to simplify the notation, the italic $\mathit{\Omega} = [\underline{\omega}, \overline{\omega}]$ denotes the band $\Omega = [-\overline{\omega}, -\underline{\omega}] \cup [\underline{\omega}, \overline{\omega}]$ with $0 \leq \underline{\omega} < \overline{\omega} \leq \pi$. In Figure 1, for each band we show the normalized band spectrum covariance matrix $\mathcal{C}_0(\mathit{\Omega}) = 0.5(\overline{\omega} - \underline{\omega})^{-1} \mathbf{C}_0(\mathit{\Omega})$ of our dataset with variables grouped by five broad categories.[20] All in all, stronger comovements are visible as lower frequencies are considered — this is particularly evident for housing variables. So, while Granger (1966) described a typical spectral shape for which the long cycles are relatively more important in the (univariate) spectra of economic variables, we find that the strength of comovements among economic variables has a similar pattern. Other interesting patterns emerge from this picture such as the nearly constant covariances over all bands of "money and credit variables", and the covariance within the "prices" category, which is somewhat stronger at the two extreme bands $\mathit{\Omega}_1$ and $\mathit{\Omega}_4$.

In order to shed more light on the eigenstructure of the data, we now analyze if factor estimates within spectral bands differ from their full spectra counterpart, as usual estimated via principal components. As discussed in Section 2.2.1, in absence of frequency-specific effects factors estimated at different frequency bands are estimates of full-spectra factors (see also the simulation evidence in Appendix A). In Table 1 we report trace-R^2 statistics $R^2\left(\hat{\mathbf{F}}(\mathit{\Omega}_i), \hat{\mathbf{F}}\right)$ as in equation (23) for $i = 1, \ldots, 4$, where $\hat{\mathbf{F}}(\mathit{\Omega}_i)$ is a $T \times r$-dimensional matrix of band spectrum principal components and $\hat{\mathbf{F}}$ (full-spectra) principal components. These results show that principal component estimates vary across bands of frequencies and the usual full-spectrum estimator is dominated by high-frequency comovements. The trace-R^2 between our lowest frequency BSPC and PC estimates takes values which are similar to those we found in the simulation exercise in presence of frequency-specific factors (see Appendix A.2).

[19]For a given vintage, we define as outliers observations with absolute value larger than 6 times the interquartile distance and replace them with the median, where both interquantile distance and median are calculated from the empirical density in that vintage.

[20]The normalization by the size of the band gives comparable covariances $\mathcal{C}_0(\mathit{\Omega})$s across bands of different sizes. Their non-normalized counterparts $\mathbf{C}_0(\mathit{\Omega})$s are, instead, the components of $\mathbf{C}_0$ due to the fluctuations in different bands. For example, with our chosen bands we have $\mathbf{C}_0 = \sum_{i=1}^4 \mathbf{C}_0(\mathit{\Omega}_i) = \sum_{i=1}^4 2(\overline{\omega}_i - \underline{\omega}_i)\mathcal{C}_0(\mathit{\Omega}_i)$.

While these results cast some doubts on the lack of frequency-specific effects, this is far from being clear-cut evidence. Most importantly, this preliminary analysis of our macroeconomic dataset is not insightful on the predictive power of (BS)PC for excess bond returns.

4. Excess bond returns forecasts

We forecast nonoverlapping excess bond returns (13) one month ahead via usual predictive regressions of the type

$$\hat{rx}_{t+1}^{(n)} = \hat{\alpha} + \hat{\beta}\hat{F}_t\left(\Omega, \mathbf{z}\right) \tag{14}$$

where $\hat{F}_t\left(\Omega, \mathbf{z}\right)$ is a supervised band spectrum principal component obtained as in equation (11) for some choice of Ω and $\mathbf{z}$ to be discussed below.[21]

Our predictions are obtained estimating the forecasting equation (14) over an expanding window, that is, at time t we use all past data available in real time t which, as explained in Section 3.2, generally means using observations up to month $t-2$ or $t-1$.

Our first prediction is made at the time of our first vintage of April 1982 to predict the excess bond returns in May 1982 and so on until the last prediction made using the November 2020 vintage to predict the excess bond returns in December 2020. Denoting T_0 the time corresponding to April 1982 and T that corresponding to December 2020, our out-of-sample forecasts are made in real time $t = T_0, T_0+1, \ldots, T-1$.

The methodology described in Section 2, is based on two key choices: a band of frequencies $\mathit{\Omega}$ for our frequency-specific factors, and a vector of proxies $\mathbf{z}$ for the predictive signal in the common macroeconomic cycles corresponding to the frequencies in $\mathit{\Omega}$. Similarly in spirit to previous works on frequency-, horizon- or scale-specific effects, in order to dissect the predictability of excess bond returns we explore different choices of $\mathit{\Omega}$. For example, Bandi et al. (2019) study scale-specific predictability in predictive regressions under temporal aggregation over different horizons. In order to observe whether the predictive power of common macroeconomic cycles varies across frequency bands, we consider the bands $\mathit{\Omega}_1$, $\mathit{\Omega}_2$, $\mathit{\Omega}_3$, $\mathit{\Omega}_4$, as defined in Section 3.2.

For each band $\mathit{\Omega}_i$, $i = 1, \ldots, 4$, we consider two alternative vectors of proxies $\mathbf{z}_t$, both including the average excess bond return across maturities $\bar{rx}_{t+1} = \frac{1}{9}\sum_{n=2}^{10} rx_{t+1}^{(n)}$.

$\mathbf{z}_t^{Infl} = (infl_t,\ \bar{rx}_{t+1})'$, where $infl_t = (1-L)^2\, CPI_t$ and CPI_t is the "Consumer Price Index for All Urban Consumers: All Items" taken from the ALFRED dataset.[22]

$\mathbf{z}_t^{Tms} = (tms_t,\ \bar{rx}_{t+1})'$, where tms_t is the term spread taken from the dataset of Welch and Goyal (2008).

[21] The estimation of the spectral density matrix in equation (9) is defined with a bandwidth equal to the smallest integer near to the square root of the sample size. As explained in Section 3.2, publication delays dictate the actual sample size available for our expanding estimation in real time t. Hence, our bandwidth becomes $\lfloor\sqrt{\mathcal{T}_t}\rfloor$ where $\mathcal{T}_t$ is the actual sample size at time t.

[22] Since CPI is part of our macroeconomic dataset, using it as a proxy means removing it from the panel $\mathbf{X}$ before the estimation of factors. Clearly, not doing so would yield a panel of projected data $\hat{\mathbf{X}}$ with a singular convariance matrix.

As discussed in Section 2.3, the supervised learning literature suggests the target variable to be predicted as a natural proxy for the central subspace. Since, following Cochrane and Piazzesi (2005), the same factors are used to predict excess bond returns across all maturities, in both choices above we consider the "average target" $\bar{rx}_{t+1}$ rather than each target $rx^{(n)}_{t+1}$. Of course, since $\bar{rx}_{t+1}$ leads the predictors x_{it}, these choices mean that at time t the projections $\hat{x}_{it}(\mathbf{z}) = \mathrm{Proj}(x_{it}|\mathbf{z}_t)$ can be estimated up to time $t-1$. Inflation and term spread are well-known predictors of excess returns since at least Fama (1981) and Fama and French (1989) and our choice is consistent with term structure models such as that of Cieslak and Povala (2015).

In order to reach a conclusion regarding the existence of frequency-specific effects, we also make predictions based on full-spectrum principal components of projected data corresponding to $\Omega_0 = [0,\ \pi]$ for which cycles of all lengths are aggregated.

For $i = 0, 1, \ldots, 4$, the predictions obtained using the predictor $\hat{F}_t\left(\Omega_i, \mathbf{z}^{Infl}\right)$ in the forecasting equation (14) are denoted as $Infl(\Omega_i)$, while $Tms(\Omega_i)$ stands for the predictions using $\hat{F}_t\left(\Omega_i, \mathbf{z}^{Tms}\right)$.

4.1. Statistical accuracy

We compare our forecasts against the standard benchmark suggested by the expectations hypothesis, the historical mean $\hat{rx}^{(n)}_{t+1,EH}$. Following Campbell and Thompson (2008), we use the out-of-sample R^2 measure

$$R^2_{OS} = 1 - \frac{\sum_{t=T_0+1}^{T}\left(\hat{rx}^{(n)}_t - rx^{(n)}_t\right)^2}{\sum_{t=T_0+1}^{T}\left(\hat{rx}^{(n)}_{t,EH} - rx^{(n)}_t\right)^2} \tag{15}$$

that is, a relative reduction in mean square error, which in all tables is reported in percentages. Following the standard practice in this literature, we evaluate the statistical significance of these mean square error improvements using the test of Clark and West (2006).

The R^2_{OS} values in Table 2 support the existence of frequency-specific predictors as the forecasts corresponding to the bands Ω_2, Ω_3 and Ω_4 are considerably more accurate than those corresponding to Ω_1 and the full spectrum Ω_0. This suggests that high-frequency macroeconomic fluctuations are noisy and add measurement error to the predictors.

Starting from the forecasts obtained using the vector of proxies $\mathbf{z}^{Infl}_t$, while the R^2_{OS}s of $Infl(\Omega_0)$ and $Infl(\Omega_1)$ are either negative or insignificant at all maturities, $Infl(\Omega_2)$, $Infl(\Omega_3)$, $Infl(\Omega_4)$ provide large R^2_{OS}s at all maturities which are 1% significant at maturities 2 to 6 and 5% significant at maturities 7 to 10. Also, the R^2_{OS}s of $Infl(\Omega_2)$, $Infl(\Omega_3)$, $Infl(\Omega_4)$ are larger at shorter maturities. Overall, $Infl(\Omega_4)$ is slightly more accurate than $Infl(\Omega_2)$ and $Infl(\Omega_3)$ at each maturity.

Much statistical significance is found across all bands when $\mathbf{z}^{Tms}_t$ is used as proxy. However, 1% significance at all maturities is only found for $Tms(\Omega_2)$, $Tms(\Omega_3)$ and $Tms(\Omega_4)$.

Furthermore, $Tms(\Omega_0)$ and $Tms(\Omega_1)$ are associated with smaller R^2_{OS}s at all maturities and considerably so for maturities of at least 3 years. $Tms(\Omega_2)$, $Tms(\Omega_3)$ and $Tms(\Omega_4)$ provide their largest R^2_{OS}s at maturities longer than 3 years.

These results provide evidence of frequency-specific predictability which vanishes completely or becomes weaker when full-spectrum predictors are used. In Appendix C (Table C.1) we show that even adopting the supervised learning approaches of Huang et al. (2023) and Fan et al. (2017) (which, as discussed in Section 2.3, are related to ours) full-spectrum predictors perform poorly. Regarding the real-time forecasting performance of unsupervised principal component predictors, we refer to Wan et al. (2022) who find no evidence of predictability for nonoverlapping returns. Finally, in unreported results (available upon request), we find that unsupervised frequency-specific factors are also not accurate. This confirms the results of Ludvigson and Ng (2009) who document the existence of common macroeconomic variation unrelated to bond return predictability.

4.2. Economic value of the forecasts

Thus far we found statistical evidence of bond return predictability using frequency-specific factors. However, as pointed out by works such as Thornton and Valente (2012) and Sarno et al. (2016), statistically accurate forecasts do not necessarily generate economic value for investors trading on Treasury bonds. Therefore, we now examine whether our forecasts translate into economic gains for investors with mean-variance preferences or a power utility function. In both cases, we consider the asset allocation decisions of an investor who selects weights $w_t^{(n)}$ on a risky bond with n years to maturity versus the one-month T-bill, that is a risk-free yield $y_t^{(1/12)}$.

A mean-variance investor maximizes the utility function

$$U\left(w_t^{(n)}, rx_{t+1}^{(n)}\right) = E_t\left(R_{p,t+1}^{(n)}\right) - \frac{\gamma}{2}\mathrm{Var}_t\left(R_{p,t+1}^{(n)}\right) \tag{16}$$

where γ is the relative risk aversion and $R_{p,t+1}^{(n)} = y_t^{(1/12)} + w_t^{(n)} rx_{t+1}^{(n)}$ the portfolio return at time $t+1$ given the generic allocation $w_t^{(n)}$. The solution of the above optimisation problem is

$$\dot{w}_t^{(n)} = \frac{\hat{rx}_{t+1}^{(n)}}{\gamma\left(\hat{\sigma}_{t+1|t}^{(n)}\right)^2}$$

where $\hat{rx}_{t+1}^{(n)}$ is some excess return forecast on n-year bond, and $\left(\hat{\sigma}_{t+1|t}^{(n)}\right)^2$ is the conditional variance estimated using a rolling window estimator over the past five years of observations as in Campbell and Thompson (2008).

A power utility investor instead maximizes the utility function

$$U\left(w_t^{(n)}, rx_{t+1}^{(n)}\right) = \frac{1}{1-\gamma}\left(\left(1-w_t^{(n)}\right)\exp\left(y_t^{(1/12)}\right) + w_t^{(n)}\exp\left(y_t^{(1/12)} + rx_{t+1}^{(n)}\right)\right)^{1-\gamma} \tag{17}$$

In this case, the optimal weights we use are those obtained under the log-normal approximation of Campbell and Viceira (1999)

$$\dot{w}_t^{(n)} = \frac{\hat{rx}_{t+1}^{(n)} + \left(\hat{\sigma}_{t+1|t}^{(n)}\right)^2/2}{\gamma\left(\hat{\sigma}_{t+1|t}^{(n)}\right)^2}$$

Under both preferences, we follow Campbell and Thompson (2008) who winsorize the weights by imposing the restriction $0 \leq w_t^{(n)} \leq 1.5$ to prevent the investor from taking extreme positions such as leveraging above 150% and shorting positions.

The optimal portfolio weights $\dot{w}_t$ given some predictions $\hat{rx}_{t+1}^{(n)}$ are used at every time t to compute the investor's realized utilities $\dot{U}_{t+1}$. Similarly, the benchmark realized utilities $\dot{U}_{t+1,EH}$ are obtained using optimal weights given the expectations hypothesis forecasts $\hat{rx}_{t+1,EH}^{(n)}$. The certainty equivalent return (CER) gains of a given predictive model with respect to the benchmark are obtained as the difference between its average realized utility over time and the average benchmark realized utility. So, positive CER gains indicate that the predictive model considered produces economic value in excess of that of the expectations hypothesis model. We report CER gains in annualized percentage terms. Finally, to test whether these gains are statistically greater than zero, we use the test of Diebold and Mariano (1995). Specifically, we estimate the regression

$$\dot{U}_{t+1}^{(n)} - \dot{U}_{t+1,EH}^{(n)} = \delta^{(n)} + \epsilon_{t+1}^{(n)}$$

and test if $\delta^{(n)}$ equals zero. To examine the effect of risk aversion γ, we repeat the above analysis considering the values 3, 5 and 8.

Table 3 shows the CER gains for investors with mean-variance utility. The most important result here is the evidence of significant CER gains which thus far, to the best of our knowledge, has not been found with nonoverlapping returns using data available in real-time. However, no single predictor provides significant CER gains at all maturities and across all risk aversion coefficients. For example, no prediction is significant at maturities 9 and 10 when $\gamma = 8$.

Similarly to the R^2_{OS}s in Section 4.1, when $\mathbf{z}_t^{Infl}$ is used we find evidence of frequency-specific effects with results varying much across our spectral bands. Regardless the risk aversion coefficient, all CER gains of $Infl\,(\Omega_0)$ and $Infl\,(\Omega_1)$ are either negative or insignificant. The CER gains of $Infl\,(\Omega_2)$, $Infl\,(\Omega_3)$ and $Infl\,(\Omega_4)$ are instead significant across all maturities for $\gamma = 3$, until maturity 8 for $\gamma = 5$, and until maturity 6 for $\gamma = 8$. At least for $\gamma = 5, 8$, $Infl\,(\Omega_4)$ is slightly better than $Infl\,(\Omega_2)$ and $Infl\,(\Omega_3)$.[23]

Some interesting patterns across our spectral bands emerge when $\mathbf{z}_t^{Tms}$ is used. For all risk aversion coefficients, $Tms\,(\Omega_1)$ gives significant CER gains at maturities 2 to 6 and insignificant gains at maturities 8 to 10. $Tms\,(\Omega_2)$ has the largest (significant) CER gains at maturities 7 to 10 for risk aversion $\gamma = 3, 5$, and at maturities 5 to 8 for $\gamma = 8$. Despite being outperformed by

[23] Among $Infl\,(\Omega_2)$, $Infl\,(\Omega_3)$, $Infl\,(\Omega_4)$, the latter is the only one to exceed the others at some maturities by at least 0.01 and at the same or higher levels of significance.

$Tms\,(\Omega_2)$, $Tms\,(\Omega_3)$, $Tms\,(\Omega_4)$ in statistical terms, $Tms\,(\Omega_0)$ generates some significant CER gains, especially at the two shortest maturities, 2 and 3.

At least qualitatively, the results are very similar for power utility investors; the corresponding CER gains are reported in Appendix C (Table C.2).

4.3. Two predictors and the spanning hypothesis

In the previous sections we found considerable differences between forecasts obtained across different bands of frequencies both in statistical and economic terms. This is true for both families of predictors $\hat{F}_t\left(\Omega, \mathbf{z}^{Infl}\right)$ and $\hat{F}_t\left(\Omega, \mathbf{z}^{Tms}\right)$ as Ω varies between the bands Ω_1 to Ω_4. Nonetheless, $Tms\,(\Omega)$ predictions are better when shorter common macroeconomic cycles are considered and are relatively more accurate for bonds with longer maturities, while the opposite applies to $Infl\,(\Omega)$. So, we are tempted to conjecture that $\mathbf{z}^{Infl}$ and $\mathbf{z}^{Tms}$ proxy for different predictable components of excess bond returns.

Searching for more convincing evidence, we now extend our out-of-sample predictive exercise by considering the following additional predictive models based on two predictors

$$\hat{rx}_{t+1}^{(n)} = \hat{\alpha} + \hat{\beta}_1 \hat{F}_t\left(\Omega_i, \mathbf{z}^{Infl}\right) + \hat{\beta}_2 \hat{F}_t\left(\Omega_j, \mathbf{z}^{Tms}\right) \tag{18}$$

for any possible pair of predictors for $i, j = 0, 1, \ldots, 4$. For each pair we make forecasts and in Figure 2 we report averages across maturities of R^2_{OS} values and CER gains under mean-variance preferences. These results show that the most accurate individual predictors combine well together. In line with the above results on $Infl\,(\Omega_4)$ and $Tms\,(\Omega_2)$, the predictions based on both predictors $\hat{F}_t\left(\Omega_4, \mathbf{z}^{Infl}\right)$ and $\hat{F}_t\left(\Omega_2, \mathbf{z}^{Tms}\right)$ yield the largest average R^2_{OS} and average CER gains for all risk aversion coefficients. Also, similarly to the evidence on individual predictors, full-spectrum predictions — corresponding to the pair $\hat{F}_t\left(\Omega_0, \mathbf{z}^{Infl}\right)$, $\hat{F}_t\left(\Omega_0, \mathbf{z}^{Tms}\right)$ — or those based on the shortest macroeconomic cycles are less accurate.[24] Again, R^2_{OS}s and CER gains vary much across the bands of frequencies considered. $\hat{F}_t\left(\Omega, \mathbf{z}^{Infl}\right)$ gives much better results at Ω_2, Ω_3, Ω_4, that is when higher-frequency fluctuations are excluded. $\hat{F}_t\left(\Omega, \mathbf{z}^{Tms}\right)$ is more accurate at Ω_2, especially in terms of CER gains.

In Table 4, for each maturity we report all results — R^2_{OS} values and CER gains — based on the forecasts jointly produced by our most accurate predictors $\hat{F}_t\left(\Omega_4, \mathbf{z}^{Infl}\right)$ and $\hat{F}_t\left(\Omega_2, \mathbf{z}^{Tms}\right)$ using the forecasting equation (18) for $i = 4$ and $j = 2$. We label such forecasts as *Both*. In Panel A of Table 4 we see that *Both* gives R^2_{OS} values which are considerably larger than $Infl\,(\Omega_4)$ and $Tms\,(\Omega_2)$ (or any other prediction obtained with a single predictor) and 1% significant at all maturities. The evidence in Panel B of Table 4 is even stronger since, unlike any forecast based on individual predictors, *Both* gives significant CER gains at all maturities

[24] Despite positive averages across maturities, in unreported results (available upon request), we found that the full-spectrum pair $\hat{F}\left(\Omega_0, \mathbf{z}^{Infl}\right), \hat{F}\left(\Omega_0, \mathbf{z}^{Tms}\right)$ and the pair at our highest-frequency band $\hat{F}\left(\Omega_1, \mathbf{z}^{Infl}\right), \hat{F}\left(\Omega_1, \mathbf{z}^{Tms}\right)$ provide little evidence of significant CER gains across maturities and risk aversion coefficients.

and for any value of risk aversion. This strengthens our novel result of significant CER gains using nonoverlapping returns and data available in real time: *Both* forecasts are our best both in economic and statistical terms. We must conclude that $\hat{F}_t\left(\Omega_4, \mathbf{z}^{Infl}\right)$ and $\hat{F}_t\left(\Omega_2, \mathbf{z}^{Tms}\right)$ are two powerful predictors for different predictive components of excess bond returns. In the rest of this paper we refer to them as *inflation factor* and *term spread factor*, respectively.

The results discussed thus far do not help understanding whether excess bond return predictability comes uniquely from the information contained in the current yield curve as the *spanning hypothesis* postulates. While, by construction, the term spread factor is a spanned factor related to the slope of the current yield curve, our inflation factor could contain information which is unspanned by the cross-section of yields. In order to determine if that is the case, we need to obtain an unspanned version of the inflation factor. We do so by controlling for yields variation in the estimation of the inflation factor. In our algorithm (Section 2.3) we now replace $\hat{\mathbf{X}}_t(\mathbf{z})$ with $\tilde{\mathbf{X}}_t(\mathbf{z}) = \{\tilde{x}_{it}(\mathbf{z}), i = 1, \ldots, N\}$ where $\tilde{x}_{it}(\mathbf{z}) = \delta'_{i,z}\mathbf{z}_t$ is the unspanned component of x_{it} using some controls for yields $\mathbf{c}_t$ in the projection $\text{Proj}\left(x_{it}|\mathbf{z}_t, \mathbf{c}_t\right) = \delta'_{i,z}\mathbf{z}_t + \delta'_{i,c}\mathbf{c}_t$.[25] We repeat this exercise with four different controls for yields: the Cochrane-Piazzesi factor ($\mathbf{c}_t^{(1)}$), 3 and 5 principal components of yields ($\mathbf{c}_t^{(2)}$ and $\mathbf{c}_t^{(3)}$), and our term spread factor (now $\mathbf{c}_t^{(4)}$). The R^2_{OS} values in Table 5 show that these four unspanned versions of our original inflation factor $\hat{F}_t\left(\Omega_4, \mathbf{z}^{Infl}\right)$ generate predictions which are as accurate as those generated by the original factor (already seen in Table 2 and repeated in the last line of Table 5 for readability). Therefore, all the predictive content of the inflation factor must reside in its unspanned component. These results imply that affine term structure models should include macroeconomic unspanned information which, similarly to Ludvigson and Ng (2009), Chernov and Mueller (2012), Joslin et al. (2014), Coroneo et al. (2016), relates to the inflation.

5. Links to the real economy

5.1. Monetary policy

Being particularly accurate at the short end of the yield curve and containing unspanned macroeconomic information, the inflation factor must be closely related with monetary policy. At the same time, since it maximises cycles of at least 8 years, the inflation factor must be associated with an endogenous component of monetary policy with permanent effects in the economy, not the typically transitory monetary policy shock. This suggest that the inflation factor is linked to systematic monetary policy, especially inflation targeting. We corroborate this intuition by estimating predictive regressions where the inflation factor is found to predict survey measures of inflation expectations taken from the Survey of Professional Forecasters. In Table 6, we show that this result holds even taking into account lagged expected inflation or lagged observed inflation. This means that the inflation factor predicts survey inflation expectations no matter

[25] An alternative procedure would be to first project the x_{it}'s onto $\mathbf{c}_t$ and then estimate the inflation factor using the residuals of such projection. The results are very similar to those in Table 5.

whether agents adjust their expectations just sluggishly or learn from their mistakes.

Bianchi et al. (2022) (BLL henceforth) propose a macro-finance model of monetary policy transmission documenting that long-lasting effects of monetary policy are due to changes in the stance of monetary policy. *Hawkish* regimes, in which the monetary policy rule of the Federal Reserve becomes more responsive to inflation, are associated with increased return premia. The main intuition is that hawkish monetary policy widens the *monetary policy spread*, the gap between the real federal fund rate and the natural rate. BLL find two hawkish regimes in the US: the first starts before the beginning of our forecasted sample (i.e. the last quarter of 1978) and ends in the third quarter of 2001, the second spans 2006:Q2 to 2008:Q2.

Is our inflation factor consistent with BLL's evidence? We analyse the predictions obtained using the inflation factor by decomposing our statistical and economic measures of predictability across BLL's hawkish and dovish regimes of monetary policy. R^2_{OS} and CER gains are reported in Table 7 (Panel A and B, respectively). Both measures provide clear-cut results. At all maturities, R^2_{OS} and CER gains are positive and highly significant during hawkish regimes while they turn negative during dovish regimes. In Figure 3 we plot the cumulative utility gains averaged across maturities in our baseline mean-variance exercise with $\gamma = 5$ (blue line) together with BLL's smoothed probability of hawkish monetary policy. The figure shows that the economic value generated by the inflation factor moves in sync with the regimes of monetary policy — positive during hawkish regimes (cumulative utility gains increase) and negative during dovish regimes (cumulative utility gains decrease) — seemingly sharing the same turning points. To validate this visual intuition we adopt the test of directional predictive ability proposed by Pesaran and Timmermann (1992). Under the null hypothesis the inflation factor does not predict the turning points of the monetary policy spread which in BLL's model drives regime switches in the stance of the Federal Reserve. Such null hypothesis is rejected with a p-value equal to 0.027. We must conclude that the stance of monetary policy is indeed a key component of the inflation factor.

5.2. Business-cycle risk

We now turn to the term spread factor. Considering that it maximizes macroeconomic cycles of 1 to 3 years, and its association with the term spread, it seems intuitive that the term spread factor represents investors' perception of business-cycle risk. In order to validate this interpretation, we begin by investigating whether the term spread predicts recessions. In Panel A of Table 8 we show that it predicts monthly and annual changes of the (monthly) smoothed US recession probability, and quarterly and annual changes of the (quarterly) GDP-based recession indicator index. So, our term spread factor is a leading business-cycle indicator just like the term spread. Going back to return predictability, in Panel B of Table 8 we show that the term spread factor is a powerful predictor of nonoverlapping bond returns, while the term spread is a much weaker predictor. We run three return predictive regressions at each maturity: in the first one we include both term spread factor and term spread, in the second one only the term spread, in the last one only the term spread factor. Two results are noteworthy. First, the term spread does not contain any predictive information which is not already in our term spread factor. Second, at least at longer maturities, the term spread contains some predictive power for nonoverlapping bond returns, while the term spread factor is a strong predictor at all maturities. Taken together, this evidence sheds light on the benefits of our supervised learning approach when we use the term spread as a proxy of expected returns. Since it predicts recessions, the term spread factor explains the link between the business-cycle and the slope of the yield curve. At the same time, such business-cycle information is effectively exploited by our BSPC estimator to extract from a number of macroeconomic indicators a predictive signal for bond returns which is way more powerful than that contained in the term spread.

We continue our analysis by observing the performance of the term spread factor over our sample. Unlike the inflation factor, whose economic value is confined to short subsamples (hawkish policy regimes), the term spread factor generates more consistent economic value over time; see the cumulative utility gains in Figure 4. We now split our sample into periods of recessions and expansions using the NBER recession indicator.[26] In Table 9 we decompose the R^2_{OS} of the predictive models based on our two factors either individually ($Infl\,(\Omega_4)$ and $Tms\,(\Omega_2)$) or jointly ($Both$). Most predictability is found in recessions. However, unlike a number of works concluding that return predictability is absent during expansions — among many others see Rapach and Zhou (2013), Henkel et al. (2011), Dangl and Halling (2012) for equity returns, and Sarno et al. (2016); Gargano et al. (2019) for bond returns —, we find evidence of predictability even in expansions which is entirely accounted for by the term spread factor. Predictability during expansions is also found by Bianchi et al. (2021) who also use machine learning techniques, albeit different from ours, and by Andreasen et al. (2021).

The results in Table 9 bear two remarkable similarities with Andreasen et al. (2021) who study the predictive performance of the slope of the yield curve across the business cycle. First, the term spread is powerful during expansions. Indeed, while the forecasts obtained without including the term spread factor ($Infl\,(\Omega_4)$) generate negative R^2_{OS} in expansions at most maturities, $Tms\,(\Omega_2)$ and $Both$, which include the term spread factor, give 1%-significant improvements over the benchmark at all maturities. Second, the predictive power of the term spread factor gets weaker in recessions for longer maturities. During recessions the $Tms\,(\Omega_2)$ forecasts, based only of the term spread factor, are just 10%-significant for maturities up to 6 years and insignificant at longer maturities.

There are important portfolio implications if the term spread factor accounts for investors hedging against business-cycle risk. In Table 10 we report CER gains in expansions and recessions. These results show that the term spread factor is a hedge in recession as investors demand compensation for exposure to it only during expansions. That is, during recessions investors are willing to get exposure to a term spread factor, while in expansions the term spread factor becomes a usual risk factor. Using a macro-finance term structure model, Andreasen et al. (2021) conclude that this result is due to accommodating monetary policy in recessions as investors

[26]The recession indicator “USREC”, is taken from the FRED database.

perceive the ability of the Federal Reserve to stimulate the economy and close the output gap.

5.3. Additional results on business cycles

Motivated by the intuition that investors demand compensation for the risk of recessions, notable rational expectations models, such as Campbell and Cochrane (1999) and Wachter (2006), feature countercyclical risk aversion. Having established evidence of predictability, we now investigate whether our out-of-sample expected returns are consistent with the countercyclical risk premia widely documented by prior empirical works dismissing the expectations hypothesis such as Fama and Bliss (1987) and Campbell and Shiller (1991).

We start by measuring whether our expected returns correlate with monthly measures of real economic activity growth. Table 11 shows that expected returns generated by our two factors either individually ($Infl\,(\Omega_4)$ and $Tms\,(\Omega_2)$) or jointly ($Both$) are clearly countercyclical. All these forecasts are negatively correlated with the Michigan consumer sentiment index (MCSI) and significantly so at 1% for all maturities. Evidence of countercyclicality is also found by looking at the year-on-year industrial production growth (IP y-o-y growth) and the Chicago Fed National Activity sub-index on consumption and housing (CFNAI C&H). The only exception is the correlation between $Tms\,(\Omega_2)$ and IP y-o-y growth which is still negative but insignificant. The absolute value of all correlations increases across maturities. The same conclusion is reached by adjusting for risk: in Appendix C we report larger Sharpe ratios during recessions than expansions for all maturities and predictions (see Table C.3).

Additional evidence in line with countercyclical risk aversion comes from Table 9 which shows that accuracy in recessions (measured by R^2_{OS}s) is way higher than during expansions, and Table 10 where we observe larger economic value (CER gains) during recessions. In Appendix C, we report countercyclical term premium estimates adopting the method of Ludvigson and Ng (2009).

6. Conclusions

Real-time macroeconomic data can predict nonoverlapping excess bond returns and generate economic value for investors. However, a spectral method is needed because their predictive power is only related to common macroeconomic cycles of specific lengths. Thanks to our band spectrum principal component approach, we find two powerful predictors: an inflation factor related to common macroeconomic cycles of at least 8 years, and a term spread factor related to cycles of 1 to 3 years. These factors have a clear economic interpretation. The inflation factor reveals a link between bond yields and Federal Reserve's inflation targeting: investors demand compensation for exposure to hawkish monetary policy. The term spread factor tracks investors' perception of business-cycle risk and their hedging strategy.

In this paper, we proposed a method to estimate latent factors when loadings vary across frequencies. Our approach is of independent interest in finance (see, for example, Huang, 2023; Li, 2024, for cross-sectional asset pricing) and macroeconomics. A more systematic approach for the detection of frequency-specific effects is left to future research.

The investigation of the international implications of our evidence is also high in our research agenda. Despite the central role of the United States in highly-integrated financial markets, business cycle synchronization, monetary policy spillovers and investors' home bias should be carefully considered in an analysis whose goals go beyond the scope of this paper.

References

Andreasen, M. M., T. Engsted, S. V. Møller, and M. Sander (2021). The Yield Spread and Bond Return Predictability in Expansions and Recessions. *Review of Financial Studies 34*(6), 2773–2812.

Atanasov, V., S. V. Møller, and R. Priestley (2020). Consumption Fluctuations and Expected Returns. *The Journal of Finance 75*(3), 1677–1713.

Bai, J. and S. Ng (2002). Determining the Number of Factors in Approximate Factor Models. *Econometrica 70*(1), 191–221.

Bai, J. and S. Ng (2008). Forecasting economic time series using targeted predictors. *Journal of Econometrics 146*(2), 304–317.

Bai, J. and S. Ng (2020). Simpler proofs for approximate factor models of large dimensions. arXiv working paper 2008.00254.

Bair, E., T. Hastie, D. Paul, and R. Tibshirani (2006). Prediction by Supervised Principal Components. *Journal of the American Statistical Association 101*(473), 119–137.

Bandi, F. M., S. E. Chaudhuri, A. W. Lo, and A. Tamoni (2021). Spectral factor models. *Journal of Financial Economics 142*(1), 214–238.

Bandi, F. M., B. Perron, A. Tamoni, and C. Tebaldi (2019). The scale of predictability. *Journal of Econometrics 208*(1), 120–140.

Bandi, F. M. and Y. Su (2023). Conditional Spectral Methods. SSRN working Paper 4284240.

Bandi, F. M. and A. Tamoni (2022). Spectral financial econometrics. *Econometric Theory 38*(6), 1175–1220.

Bandi, F. M. and A. Tamoni (2023). Business-cycle consumption risk and asset prices. *Journal of Econometrics 237*(2).

Bauer, M. D. and J. D. Hamilton (2018). Robust Bond Risk Premia. *Review of Financial Studies 31*(2), 399–448.

Bianchi, D., M. Büchner, and A. Tamoni (2021). Bond Risk Premiums with Machine Learning. *Review of Financial Studies 34*(2), 1046–1089.

Bianchi, F., M. Lettau, and S. C. Ludvigson (2022). Monetary Policy and Asset Valuation. *The Journal of Finance 77*(2), 967–1017.

Borup, D., J. N. Eriksen, M. M. Kjær, and M. Thyrsgaard (2023). Predicting Bond Return Predictability. *Management Science*. doi.org/10.1287/mnsc.2023.4713.

Campbell, J. Y. and J. H. Cochrane (1999). By force of habit: A consumption-based explanation of aggregate stock market behavior. *Journal of Political Economy 107*(2), 205–251.

Campbell, J. Y. and R. J. Shiller (1991). Yield Spreads and Interest Rate Movements: A Bird's Eye View. *Review of Economic Studies 58*(3), 495–514.

Campbell, J. Y. and S. B. Thompson (2008). Predicting Excess Stock Returns Out of Sample: Can Anything Beat the Historical Average? *Review of Financial Studies 21*(4), 1509–1531.

Campbell, J. Y. and L. M. Viceira (1999). Consumption and Portfolio Decisions when Expected Returns are Time Varying. *Quarterly Journal of Economics 114*(2), 433–495.

Caruso, A. and L. Coroneo (2023). Does Real-Time Macroeconomic Information Help to Predict Interest Rates? *Journal of Money, Credit and Banking 55*(8), 2027–2059.

Chamberlain, G. and M. Rothschild (1983). Arbitrage, Factor Structure, and Mean-Variance Analysis on Large Asset Markets. *Econometrica 51*(5), 1281–1304.

Chaudhuri, S. E. and A. W. Lo (2018). Dynamic Alpha: A Spectral Decomposition of Investment Performance Across Time Horizons. *Management Science 65*(9), 4440–4450.

Chernov, M. and P. Mueller (2012). The term structure of inflation expectations. *Journal of Financial Economics 106*(2), 367–394.

Cieslak, A. and P. Povala (2015). Expected returns in treasury bonds. *Review of Financial Studies 28*(10), 2859–2901.

Clark, T. E. and K. D. West (2006). Using out-of-sample mean squared prediction errors to test the martingale difference hypothesis. *Journal of Econometrics 135*(1-2), 155–186.

Cochrane, J. H. and M. Piazzesi (2005). Bond Risk Premia. *American Economic Review 95*(1), 138–160.

Connor, G. and R. A. Korajczyk (1986). Performance measurement with the arbitrage pricing theory. *Journal of Financial Economics 15*(3), 373–394.

Cook, R. D. (2007). Fisher Lecture: Dimension Reduction in Regression. *Statistical Science 22*(1), 1–26.

Cook, R. D. and L. Forzani (2008). Principal Fitted Components for Dimension Reduction in Regression. *Statistical Science 23*(4), 485–501.

Cooper, I. and R. Priestley (2009). Time-varying risk premiums and the output gap. *Review of Financial Studies 22*(7), 2801–2833.

Coroneo, L., D. Giannone, and M. Modugno (2016). Unspanned Macroeconomic Factors in the Yield Curve. *Journal of Business & Economic Statistics 34*(3), 472–485.

Dangl, T. and M. Halling (2012). Predictive regressions with time-varying coefficients. *Journal of Financial Economics 106*(1), 157–181.

Dew-Becker, I. and S. Giglio (2016). Asset Pricing in the Frequency Domain: Theory and Empirics. *Review of Financial Studies 29*(8), 2029–2068.

Diebold, F. X. and R. S. Mariano (1995). Comparing Predictive Accuracy. *Journal of Business & Economic Statistics 13*(3), 253–263.

Engle, R. F. (1974). Band Spectrum Regression. *International Economic Review 15*(1), 1–11.

Englund, P., T. Persson, and L. E. O. Svensson (1992). Swedish business cycles: 1861–1988. *Journal of Monetary Economics 30*(3), 343–371.

Eriksen, J. N. (2017). Expected Business Conditions and Bond Risk Premia. *Journal of Financial and Quantitative Analysis 52*(4), 1667–1703.

Fama, E. F. (1981). Stock returns, real activity, inflation, and money. *American Economic Review 71*(4), 545–565.

Fama, E. F. and R. R. Bliss (1987). The information in long-maturity forward rates. *American Economic Review*, 680–692.

Fama, E. F. and K. R. French (1989). Business conditions and expected returns on stocks and bonds. *Journal of Financial Economics 25*(1), 23–49.

Fan, J., Y. Ke, and Y. Liao (2021). Augmented factor models with applications to validating market risk factors and forecasting bond risk premia. *Journal of Econometrics 222*(1), 269–294.

Fan, J., Y. Liao, and W. Wang (2016). Projected principal component analysis in factor models. *Annals of Statistics 44*(1), 219–254.

Fan, J., L. Xue, and J. Yao (2017). Sufficient forecasting using factor models. *Journal of Econometrics 201*(2), 292–306.

Fan, Y., G. Feng, A. Fulop, and J. Li (2022). Real-time macro information and bond return predictability: A weighted group deep learning approach. SSRN working paper 3517081.

Forni, M., A. Giovannelli, M. Lippi, and S. Soccorsi (2018). Dynamic factor model with infinite-dimensional factor space: Forecasting. *Journal of Applied Econometrics 33*(5), 625–642.

Forni, M., M. Hallin, M. Lippi, and L. Reichlin (2000). The Generalized Dynamic-Factor Model: Identification and Estimation. *Review of Economics and Statistics 82*(4), 540–554.

Forni, M., M. Hallin, M. Lippi, and P. Zaffaroni (2017). Dynamic factor models with infinite-dimensional factor space: Asymptotic analysis. *Journal of Econometrics 199*(1), 74–92.

Gargano, A., D. Pettenuzzo, and A. Timmermann (2019). Bond Return Predictability: Economic Value and Links to the Macroeconomy. *Management Science 65*(2), 508–540.

Ghysels, E., C. Horan, and E. Moench (2018). Forecasting through the Rearview Mirror: Data Revisions and Bond Return Predictability. *Review of Financial Studies 31*(2), 678–714.

Giannone, D., L. Reichlin, and D. Small (2008). Nowcasting: The real-time informational content of macroeconomic data. *Journal of Monetary Economics 55*(4), 665–676.

Giglio, S., D. Xiu, and D. Zhang (2023). Prediction when factors are weak. University of Chicago, Becker Friedman Institute for Economics Working Paper 2023-47.

Granger, C. W. J. (1966). The Typical Spectral Shape of an Economic Variable. *Econometrica 34*(1), 150–161.

Greenwood, R. and D. Vayanos (2014). Bond supply and excess bond returns. *Review of Financial Studies 27*(3), 663–713.

Gürkaynak, R. S., B. Sack, and J. H. Wright (2007). The U.S. Treasury yield curve: 1961 to the present. *Journal of Monetary Economics 54*(8), 2291–2304.

Hannan, E. J. (1963). Regression for Time Series with Errors of Measurement. *Biometrika 50*(3/4), 293–302.

Hannan, E. J. (1965). The Estimation of Relationships Involving Distributed Lags. *Econometrica 33*(1), 206–224.

Hassler, J., P. Lundvik, T. Persson, and P. Soderlind (1994). The Swedish business cycle: stylized facts over 130 years. In V. Bergstrom and A. Vredin (Eds.), *Measuring and interpreting business cycles*, pp. 9–108. Clarendon Press.

Henkel, S. J., J. S. Martin, and F. Nardari (2011). Time-varying short-horizon predictability. *Journal of Financial Economics 99*(3), 560–580.

Huang, D., F. Jiang, K. Li, G. Tong, and G. Zhou (2022). Scaled PCA: A New Approach to Dimension Reduction. *Management Science 68*(3), 1678–1695.

Huang, D., F. Jiang, K. Li, G. Tong, and G. Zhou (2023). Are bond returns predictable with real-time macro data? *Journal of Econometrics*. Forthcoming.

Huang, J. (2023). Frequency dependent risks in the factor zoo. SSRN working paper 3948519.

Huang, J.-Z. and Z. Shi (2023). Machine-learning-based return predictors and the spanning controversy in macro-finance. *Management Science 69*(3), 1780–1804.

Joslin, S., M. Priebsch, and K. J. Singleton (2014). Risk Premiums in Dynamic Term Structure Models with Unspanned Macro Risks. *Journal of Finance 69*(3), 1197–1233.

Kamara, A., R. A. Korajczyk, X. Lou, and R. Sadka (2016). Horizon Pricing. *Journal of Financial and Quantitative Analysis 51*(6), 1769–1793.

Kelly, B. T., S. Pruitt, and Y. Su (2019). Characteristics are covariances: A unified model of risk and return. *Journal of Financial Economics 134*(3), 501–524.

Li, S. (2024). Low-frequency risk factors and their fundamental drivers. SSRN working paper 4589389.

Liu, Y. and J. C. Wu (2021). Reconstructing the yield curve. *Journal of Financial Economics 142*(3), 1395–1425.

Ludvigson, S. C. and S. Ng (2009). Macro Factors in Bond Risk Premia. *Review of Financial Studies 22*(12), 5027–5067.

Neuhierl, A. and R. T. Varneskov (2021). Frequency dependent risk. *Journal of Financial Economics 140*(2), 644–675.

Ortu, F., A. Tamoni, and C. Tebaldi (2013). Long-Run Risk and the Persistence of Consumption Shocks. *The Review of Financial Studies 26*(11), 2876–2915.

Pesaran, M. H. and A. Timmermann (1992). A Simple Nonparametric Test of Predictive Performance. *Journal of Business & Economic Statistics 10*(4), 461–465.

Priestley, M. B. (1981). *Spectral analysis and time series.* New York: Academic Press.

Rapach, D. and G. Zhou (2013). Chapter 6 - Forecasting Stock Returns. In G. E. a. A. Timmermann (Ed.), *Handbook of Economic Forecasting*, Volume 2, Part A of *Handbook of Economic Forecasting*, pp. 328–383. Elsevier.

Sarno, L., P. Schneider, and C. Wagner (2016). The economic value of predicting bond risk premia. *Journal of Empirical Finance 37*, 247–267.

Stock, J. H. and M. W. Watson (2002a). Forecasting Using Principal Components From a Large Number of Predictors. *Journal of the American Statistical Association 97*(460), 1167–1179.

Stock, J. H. and M. W. Watson (2002b). Macroeconomic Forecasting Using Diffusion Indexes. *Journal of Business & Economic Statistics 20*(2), 147–162.

Thornton, D. L. and G. Valente (2012). Out-of-Sample Predictions of Bond Excess Returns and Forward Rates: An Asset Allocation Perspective. *Review of Financial Studies 25*(10), 3141–3168.

Wachter, J. A. (2006). A consumption-based model of the term structure of interest rates. *Journal of Financial Economics 79*(2), 365–399.

Wan, R., A. Fulop, and J. Li (2022). Real-time Bayesian learning and bond return predictability. *Journal of Econometrics 230*(1), 114–130.

Welch, I. and A. Goyal (2008). A Comprehensive Look at The Empirical Performance of Equity Premium Prediction. *Review of Financial Studies 21*(4), 1455–1508.

Wu, W. B. and P. Zaffaroni (2018). Asymptotic theory for spectral density estimates of general multivariate time series. *Econometric Theory 34*(1), 1–22.

Tables

Table 1: Macro data: BSPC estimates.

	r				
	1	2	3	5	8
$R^2\left(\hat{\mathbf{F}}(\Omega_1),\hat{\mathbf{F}}\right)$	0.997	0.910	0.878	0.905	0.962
$R^2\left(\hat{\mathbf{F}}(\Omega_2),\hat{\mathbf{F}}\right)$	0.953	0.941	0.904	0.935	0.904
$R^2\left(\hat{\mathbf{F}}(\Omega_3),\hat{\mathbf{F}}\right)$	0.748	0.738	0.791	0.873	0.866
$R^2\left(\hat{\mathbf{F}}(\Omega_4),\hat{\mathbf{F}}\right)$	0.617	0.713	0.773	0.849	0.850

Notes: Trace-R^2 statistics (23) for common factors estimated from the of the ALFRED dataset (December 2020 vintage). $\hat{\mathbf{F}}(\Omega_i)$ are band spectrum principal components where the bands Ω_i for $i = 1, \ldots, 4$ are defined in Section 3.2; $\hat{\mathbf{F}}$ are principal components.

Table 2: R^2_{OS} across frequency bands.

	Maturities								
	2	3	4	5	6	7	8	9	10
$Infl\,(\Omega_1)$	0.593	0.279	0.136	−0.023	−0.150	−0.047	0.027	0.027	−0.023
$Infl\,(\Omega_2)$	4.385***	3.723***	2.418***	1.948***	1.993***	1.871**	1.885**	1.653**	1.573**
$Infl\,(\Omega_3)$	4.481***	3.904***	2.606***	2.115***	2.094***	1.936**	1.936**	1.687**	1.567**
$Infl\,(\Omega_4)$	4.578***	3.990***	2.679***	2.170***	2.142***	1.987**	1.982**	1.725**	1.597**
$Infl\,(\Omega_0)$	0.568	0.200	0.074	−0.106	−0.289	−0.143	−0.059	−0.049	−0.041
$Tms\,(\Omega_1)$	0.237***	0.973***	0.625**	0.738**	0.533**	0.380**	0.316*	0.269*	0.146
$Tms\,(\Omega_2)$	0.412***	1.514***	2.033***	2.226***	2.012***	1.880***	1.774***	1.743***	1.531***
$Tms\,(\Omega_3)$	0.580***	1.457***	1.973***	2.186***	2.062***	2.035***	1.969***	1.980***	1.800***
$Tms\,(\Omega_4)$	0.564***	1.437***	1.951***	2.164***	2.044***	2.020***	1.957***	1.968***	1.792***
$Tms\,(\Omega_0)$	0.074***	0.820***	0.557***	0.748**	0.544**	0.390**	0.358**	0.309*	0.127*

Notes: $\Omega_1 = [2\pi/12, \pi]$, $\Omega_2 = [2\pi/36, 2\pi/12]$, $\Omega_3 = [2\pi/96, 2\pi/36]$, $\Omega_4 = [0, 2\pi/96]$, $\Omega_0 = [0,\ \pi]$. The predictions obtained using the predictor $\hat{F}_t\left(\Omega_i, \mathbf{z}^{Infl}\right)$ in the forecasting equation (14) are denoted as *Infl*(Ω_i) for $i = 0, 1, \ldots, 4$. *Tms*(Ω_i) stands for the same predictions using $\hat{F}_t\left(\Omega_i, \mathbf{z}^{Tms}\right)$. *, **, *** denote statistical significance at 10, 5, 1 percent level using the test of Clark and West (2006) (only reported for positive R^2_{OS} values).

Table 3: CER gains (Mean-Variance utility)

	Maturities								
	2	3	4	5	6	7	8	9	10
					$\gamma = 3$				
$Infl\,(\Omega_1)$	0.128	0.176	0.275	0.119	−0.029	−0.158	−0.206	−0.407	−0.517
$Infl\,(\Omega_2)$	0.401*	0.685**	0.806**	0.843**	0.904*	0.933*	1.194*	1.328**	1.450**
$Infl\,(\Omega_3)$	0.463*	0.749**	0.888**	0.935**	1.014*	1.061*	1.286*	1.467**	1.604**
$Infl\,(\Omega_4)$	0.457*	0.743**	0.887**	0.922**	1.017*	1.070*	1.285*	1.475**	1.622**
$Infl\,(\Omega_0)$	0.029	0.103	0.194	0.020	−0.151	−0.299	−0.318	−0.585	−0.670
$Tms\,(\Omega_1)$	0.433*	0.567*	0.496*	0.564*	0.819*	0.774	0.837	0.948	0.935
$Tms\,(\Omega_2)$	0.238	0.510*	0.699*	0.644	0.776	1.007*	1.285*	1.738**	1.888**
$Tms\,(\Omega_3)$	0.163	0.327	0.397	0.369	0.604	0.982	1.259*	1.605**	1.722**
$Tms\,(\Omega_4)$	0.156	0.317	0.391	0.352	0.586	0.966	1.241*	1.575**	1.688*
$Tms\,(\Omega_0)$	0.453*	0.579*	0.475	0.542	0.755	0.893*	1.088*	1.336**	1.374*
					$\gamma = 5$				
$Infl\,(\Omega_1)$	0.121	0.154	0.053	−0.099	−0.340	−0.439	−0.581	−0.748	−0.892
$Infl\,(\Omega_2)$	0.422*	0.653**	0.671**	0.635*	0.750*	0.907*	0.994*	0.738	0.668
$Infl\,(\Omega_3)$	0.478**	0.725**	0.745**	0.726*	0.842*	1.045**	1.129**	0.859	0.782
$Infl\,(\Omega_4)$	0.478**	0.721**	0.745**	0.741**	0.849*	1.068**	1.156**	0.888	0.811
$Infl\,(\Omega_0)$	0.079	0.116	−0.042	−0.186	−0.468	−0.582	−0.757	−0.898	−0.950
$Tms\,(\Omega_1)$	0.427*	0.489*	0.533*	0.688*	0.749*	0.839*	0.792	0.697	0.617
$Tms\,(\Omega_2)$	0.276	0.471*	0.492	0.684*	0.966*	1.442**	1.595**	1.664**	1.638**
$Tms\,(\Omega_3)$	0.158	0.232	0.271	0.506	0.742	1.174*	1.334*	1.544*	1.611*
$Tms\,(\Omega_4)$	0.150	0.227	0.263	0.493	0.725	1.146*	1.306*	1.527*	1.576*
$Tms\,(\Omega_0)$	0.427**	0.506**	0.467	0.718*	0.935**	1.064**	1.114**	1.063*	1.005
					$\gamma = 8$				
$Infl\,(\Omega_1)$	0.084	0.055	−0.093	−0.235	−0.489	−0.661	−0.707	−0.666	−0.700
$Infl\,(\Omega_2)$	0.401**	0.542**	0.443*	0.601**	0.701*	0.482	0.384	0.245	0.215
$Infl\,(\Omega_3)$	0.460**	0.601**	0.515*	0.706**	0.815**	0.596	0.476	0.303	0.274
$Infl\,(\Omega_4)$	0.462**	0.599**	0.525*	0.722**	0.835**	0.617	0.495	0.319	0.281
$Infl\,(\Omega_0)$	0.064	−0.019	−0.206	−0.381	−0.610	−0.746	−0.844	−0.803	−0.813
$Tms\,(\Omega_1)$	0.366**	0.433*	0.494*	0.632*	0.724*	0.573	0.444	0.248	0.162
$Tms\,(\Omega_2)$	0.260*	0.300	0.512*	0.910**	1.219**	1.201**	1.122*	0.866	0.645
$Tms\,(\Omega_3)$	0.130	0.096	0.308	0.664*	0.908*	1.082*	1.065	0.931	0.707
$Tms\,(\Omega_4)$	0.124	0.088	0.299	0.647*	0.890*	1.054*	1.041	0.912	0.690
$Tms\,(\Omega_0)$	0.372**	0.437*	0.573**	0.774**	0.918**	0.760	0.681	0.509	0.386

Notes: $\Omega_1 = [2\pi/12, \pi]$, $\Omega_2 = [2\pi/36, 2\pi/12]$, $\Omega_3 = [2\pi/96, 2\pi/36]$, $\Omega_4 = [0, 2\pi/96]$, $\Omega_0 = [0, \pi]$. The predictions obtained using the predictor $\hat{F}_t\left(\Omega_i, \mathbf{z}^{Infl}\right)$ in the forecasting equation (14) are denoted as $Infl(\Omega_i)$ for $i = 0, 1, \ldots, 4$. $Tms\,(\Omega_i)$ stands for the same predictions using $\hat{F}_t\left(\Omega_i, \mathbf{z}^{Tms}\right)$. *, **, *** denote statistical significance at 10, 5, 1 percent level using the test of Diebold and Mariano (1995) (only reported for positive CER gains).

Table 4: R^2_{OS} AND CER GAINS USING $\hat{F}\left(\Omega_4, \mathbf{z}^{Infl}\right)$ AND $\hat{F}\left(\Omega_2, \mathbf{z}^{Tms}\right)$

	Maturities								
	2	3	4	5	6	7	8	9	10
				Panel A: R^2_{OS}					
$Infl\,(\Omega_4)$	4.578***	3.990***	2.679***	2.170***	2.142***	1.987**	1.982**	1.725**	1.597**
$Tms\,(\Omega_2)$	0.412***	1.514***	2.033***	2.226***	2.012***	1.880***	1.774***	1.743***	1.531***
Both	5.934***	5.560***	4.495***	4.125***	4.184***	4.170***	4.056***	3.665***	3.354***
				Panel B: CER gains					
				Mean-Variance utility, $\gamma = 3$					
$Infl\,(\Omega_4)$	0.457*	0.743**	0.887**	0.922**	1.017*	1.070*	1.285*	1.475**	1.622**
$Tms\,(\Omega_2)$	0.238	0.510*	0.699*	0.644	0.776	1.007*	1.285*	1.738**	1.888**
Both	0.473*	0.717*	1.017**	1.229**	1.596**	2.064**	2.478**	2.779***	2.999***
				Mean-Variance utility, $\gamma = 5$					
$Infl\,(\Omega_4)$	0.478**	0.721**	0.745**	0.741**	0.849*	1.068**	1.156**	0.888	0.811
$Tms\,(\Omega_2)$	0.276	0.471*	0.492	0.684*	0.966*	1.442**	1.595**	1.664**	1.638**
Both	0.453*	0.649*	0.946**	1.247**	1.675**	2.185***	2.376***	2.397**	2.466**
				Mean-Variance utility, $\gamma = 8$					
$Infl\,(\Omega_4)$	0.462**	0.599**	0.525*	0.722**	0.835**	0.617	0.495	0.319	0.281
$Tms\,(\Omega_2)$	0.260*	0.300	0.512*	0.910**	1.219**	1.201**	1.122*	0.866	0.645
Both	0.433*	0.635**	0.870**	1.231**	1.603***	1.726**	1.684**	1.479*	1.370*

Notes: Forecasts labelled *Both* are obtained as in equation (18) for $i = 4$ and $j = 2$. In Panel A *, **, *** denote statistical significance at 10, 5, 1 percent level using the test of Clark and West (2006) (only reported for positive R^2_{OS} values). In Panel B *, **, *** denote statistical significance at 10, 5, 1 percent level using the test of Diebold and Mariano (1995) (only reported for positive CER gains).

Table 5: THE PREDICTIVE POWER OF THE UNSPANNED COMPONENT OF $\hat{F}_t\left(\Omega_4, \mathbf{z}^{Infl}\right)$: R^2_{OS}

	Maturities								
	2	3	4	5	6	7	8	9	10
$\mathbf{c}^{(1)}$	4.335***	4.098***	2.916***	2.342***	2.148***	1.919**	1.904**	1.663**	1.483**
$\mathbf{c}^{(2)}$	4.075***	3.848***	2.676***	2.153***	1.971***	1.724**	1.723**	1.503**	1.316**
$\mathbf{c}^{(3)}$	4.025***	3.916***	2.770***	2.205***	1.996***	1.681**	1.667**	1.473**	1.253**
$\mathbf{c}^{(4)}$	4.420***	3.754***	2.450***	2.082***	2.069***	1.944**	1.831**	1.515**	1.283**
$Infl\,(\Omega_4)$	4.578***	3.990***	2.679***	2.170***	2.142***	1.987**	1.982**	1.725**	1.597**

Notes: The R^2_{OS} reported in each line are obtained controlling for yield variation as described in Section 4.3, where the controls $\mathbf{c}^{(1)}$, $\mathbf{c}^{(2)}$, $\mathbf{c}^{(3)}$, $\mathbf{c}^{(4)}$ are the Cochrane-Piazzesi factor, 3 and 5 principal components of yields, and our term spread factor $\hat{F}_t\left(\Omega_2, \mathbf{z}^{Tms}\right)$, respectively. For readability, the R^2_{OS}s obtained with $\hat{F}_t\left(\Omega_4, \mathbf{z}^{Infl}\right)$ (rather than its unspanned component) are repeated here and denoted by $Infl\,(\Omega_4)$ as in Table 2. *, **, *** denote statistical significance at 10, 5, 1 percent level using the test of Clark and West (2006) (only reported for positive R^2_{OS} values).

Table 6: Inflation factor: in-sample predictive results

	INFCPI1YR	DPGDP3	DPGDP4	DPGDP5	DPGDP6
	$\hat{\mathrm{E}\pi}_{t+1} = \hat{\beta}\hat{F}_t\left(\Omega_4, \mathbf{z}^{Infl}\right)$				
$\hat{\beta}$	0.171**	0.431***	0.404***	0.373***	0.379***
	$\hat{\mathrm{E}\pi}_{t+1} = \hat{\beta}\hat{F}_t\left(\Omega_4, \mathbf{z}^{Infl}\right) + \hat{\delta}\mathrm{E}\pi_t$				
$\hat{\beta}$	0.037**	0.038**	0.037**	0.036**	0.020
	$\hat{\mathrm{E}\pi}_{t+1} = \hat{\beta}\hat{F}_t\left(\Omega_4, \mathbf{z}^{Infl}\right) + \hat{\delta}\pi_t$				
$\hat{\beta}$	0.167**	0.410***	0.391***	0.360***	0.368***

Notes: No intercept is included because regressors are regressands are standardized. *, **, *** denote statistical significance at 10, 5, 1 percent level. INFCPI1YR is the mean expectation of the one-year-ahead annual-average inflation measured by the CPI. DPGDP3, DPGDP4, DPGDP5 and DPGDP6 are the mean expected annualized percent change of mean GDP implicit deflator one, two, three and four quarters ahead, respectively. All variables are taken from the Survey of Professional Forecasters available at the website of the Federal Reserve Bank of Philadelphia. $\mathrm{E}\pi_t$ denotes the inflation expectation according to the corresponding column header. π_t denotes observed inflation.

Table 7: $Infl\,(\Omega_4)$: R^2_{OS} and CER gains across BLL's regimes.

	Maturities								
	2	3	4	5	6	7	8	9	10
					Panel A: R^2_{OS}				
Hawkish	8.114***	6.783***	4.731***	3.823***	3.909***	3.621***	3.452**	2.854**	2.620**
Dovish	−13.383	−6.226	−3.283	−2.073	−2.130	−1.714	−1.237	−0.632	−0.472
					Panel B: CER gains				
Hawkish	1.040**	1.557***	1.760***	2.048***	2.348***	2.610***	2.614***	2.130***	2.035**
Dovish	−0.299	−0.465	−0.733	−1.220	−1.354	−1.108	−0.845	−0.837	−0.911

Notes: In Panel A *, **, *** denote statistical significance at 10, 5, 1 percent level using the test of Clark and West (2006) (only reported for positive R^2_{OS} values). In Panel B *, **, *** denote statistical significance at 10, 5, 1 percent level using the test of Diebold and Mariano (1995) (only reported for positive CER gains). As discussed in Section 5.1, hawkish and dovish monetary policy regimes are detected as in Bianchi et al. (2022).

Table 8: Term spread factor: in-sample predictive results

Panel A: Recession probability forecasts $\Delta\hat{\mathcal{P}}_{t+1} = \hat{\beta}\hat{F}_t\left(\Omega_2, \mathbf{z}^{Tms}\right)$

	Recession indicators			
	RECPROUSM156N		JHGDPBRINDX	
	monthly	annual	quarterly	annual
$\hat{\beta}$	0.142***	0.157***	0.302***	0.349***

Panel B: return predictive regressions

	Maturities								
	2	3	4	5	6	7	8	9	10
	$\hat{rx}^{(n)}_{t+1} = \hat{\beta}^{(n)}\hat{F}_t\left(\Omega_2, \mathbf{z}^{Tms}\right) + \hat{\delta}^{(n)} tms_t$								
$\hat{\delta}^{(n)}$	−0.103	−0.066	−0.023	−0.011	−0.012	0.005	0.020	0.027	0.033
$\hat{\beta}^{(n)}$	0.242***	0.211**	0.172**	0.165**	0.176***	0.165**	0.154**	0.145**	0.138**
	$\hat{rx}^{(n)}_{t+1} = \hat{\delta}^{(n)} tms_t$								
$\hat{\delta}^{(n)}$	0.062	0.079	0.095	0.102*	0.109*	0.118**	0.125**	0.126**	0.127**
	$\hat{rx}^{(n)}_{t+1} = \hat{\beta}^{(n)}\hat{F}_t\left(\Omega_2, \mathbf{z}^{Tms}\right)$								
$\hat{\beta}^{(n)}$	0.171***	0.166***	0.157***	0.158***	0.168***	0.169***	0.168***	0.164***	0.160***

Notes: No intercept is included because regressors are regressands are standardized. *, **, *** denote statistical significance at 10, 5, 1 percent level. In Panel A, $\Delta\mathcal{P}_t$ denotes the monthly, quarterly or annual change in recession probability according to the corresponding column header. RECPROUSM156N and JHGDPBRINDX are (monthly) Smoothed US Recession probability and (quarterly) GDP-based recession indicator index, respectively, both available at the FRED database. In Panel B Newey-West standard errors are used.

Table 9: R^2_{OS} in expansions and recessions

	Maturities								
	2	3	4	5	6	7	8	9	10
	Expansions								
$Infl\,(\Omega_4)$	−1.179	0.350**	0.202*	−0.011	−0.357	−0.708	−0.642	−0.556	−0.628
$Tms\,(\Omega_2)$	0.231***	1.492***	2.023***	2.024***	1.790***	1.557***	1.566***	1.479***	1.290***
Both	0.162***	1.940***	2.131***	2.035***	1.797***	1.414***	1.439***	1.444***	1.229***
	Recessions								
$Infl\,(\Omega_4)$	20.969**	17.282***	12.847***	11.972***	14.482***	14.387**	13.494**	11.632**	10.859**
$Tms\,(\Omega_2)$	0.928*	1.599*	2.073*	3.132*	3.095*	3.335	2.634	2.829	2.464
Both	22.355**	18.774**	14.205**	13.512**	15.949**	16.805**	15.455**	13.222**	12.097**

Notes: $\Omega_2 = [2\pi/36, 2\pi/12]$, $\Omega_4 = [0, 2\pi/96]$. Forecasts labelled *Both* are obtained as in equation (18) for $i = 4$ and $j = 2$. *, **, *** denote statistical significance at 10, 5, 1 percent level using the test of Clark and West (2006) (only reported for positive R^2_{OS} values).

Table 10: CER gains in expansions and recessions

	Maturities								
	2	3	4	5	6	7	8	9	10
					Expansions				
$Infl\,(\Omega_4)$	0.260	0.425*	0.362	0.350	0.410	0.584	0.640	0.386	0.286
$Tms\,(\Omega_2)$	0.302	0.491*	0.478	0.646	0.932*	1.394**	1.558**	1.663**	1.730**
Both	0.207	0.328	0.536	0.813*	1.168*	1.656**	1.892**	2.100**	2.253**
					Recessions				
$Infl\,(\Omega_4)$	2.672*	3.708*	4.608**	4.686**	5.265**	5.941**	6.352*	5.942*	6.096*
$Tms\,(\Omega_2)$	0.017	0.279	0.647	1.101	1.345	1.896	1.832	1.468	0.426
Both	2.932*	3.877*	5.123**	5.672**	6.812**	7.474**	7.120*	5.191	4.332

Notes: $\Omega_2 = [2\pi/36, 2\pi/12]$, $\Omega_4 = [0, 2\pi/96]$. Forecasts labelled *Both* are obtained as in equation (18) for $i = 4$ and $j = 2$. CER gains are calculated as in the economic evaluation exercise described in Section 4.2 under mean-variance preferences and with $\gamma = 5$. *, **, *** denote statistical significance at 10, 5, 1 percent level using the test of Diebold and Mariano (1995) (only reported for positive CER gains).

Table 11: Macroeconomic determinants of expected excess returns

	Maturities								
	2	3	4	5	6	7	8	9	10
					IP y-o-y growth				
$Infl\,(\Omega_4)$	−0.147***	−0.149***	−0.151***	−0.151***	−0.157***	−0.165***	−0.164***	−0.172***	−0.177***
$Tms\,(\Omega_2)$	−0.052	−0.054	−0.055	−0.056	−0.056	−0.059	−0.055	−0.060	−0.063
Both	−0.106**	−0.094**	−0.079*	−0.080*	−0.094**	−0.101**	−0.097**	−0.102**	−0.109**
					CFNAI C&H				
$Infl\,(\Omega_4)$	−0.061	−0.089*	−0.133***	−0.149***	−0.132***	−0.144***	−0.141***	−0.167***	−0.176***
$Tms\,(\Omega_2)$	−0.093**	−0.106**	−0.125***	−0.142***	−0.136***	−0.154***	−0.147***	−0.167***	−0.177***
Both	−0.054	−0.073	−0.100**	−0.118**	−0.114**	−0.131***	−0.128***	−0.146***	−0.158***
					MCSI				
$Infl\,(\Omega_4)$	−0.150***	−0.158***	−0.168***	−0.170***	−0.165***	−0.170***	−0.164***	−0.173***	−0.177***
$Tms\,(\Omega_2)$	−0.256***	−0.267***	−0.277***	−0.287***	−0.283***	−0.291***	−0.284***	−0.295***	−0.301***
Both	−0.266***	−0.300***	−0.331***	−0.343***	−0.338***	−0.350***	−0.347***	−0.361***	−0.369***

Notes: Correlation between expected returns and macroeconomic cyclical indicators. IP y-o-y growth stands is the year-on-year industrial production growth, CFNAI C&H is the Chicago Fed National Activity sub-index on consumption and housing, MCSI is the Michigan consumer sentiment index. $\Omega_2 = [2\pi/36, 2\pi/12]$, $\Omega_4 = [0, 2\pi/96]$. Forecasts labelled *Both* are obtained as in equation (18) for $i = 4$ and $j = 2$. *, **, *** denote statistical significance at 10, 5, 1 percent level.

FIGURES

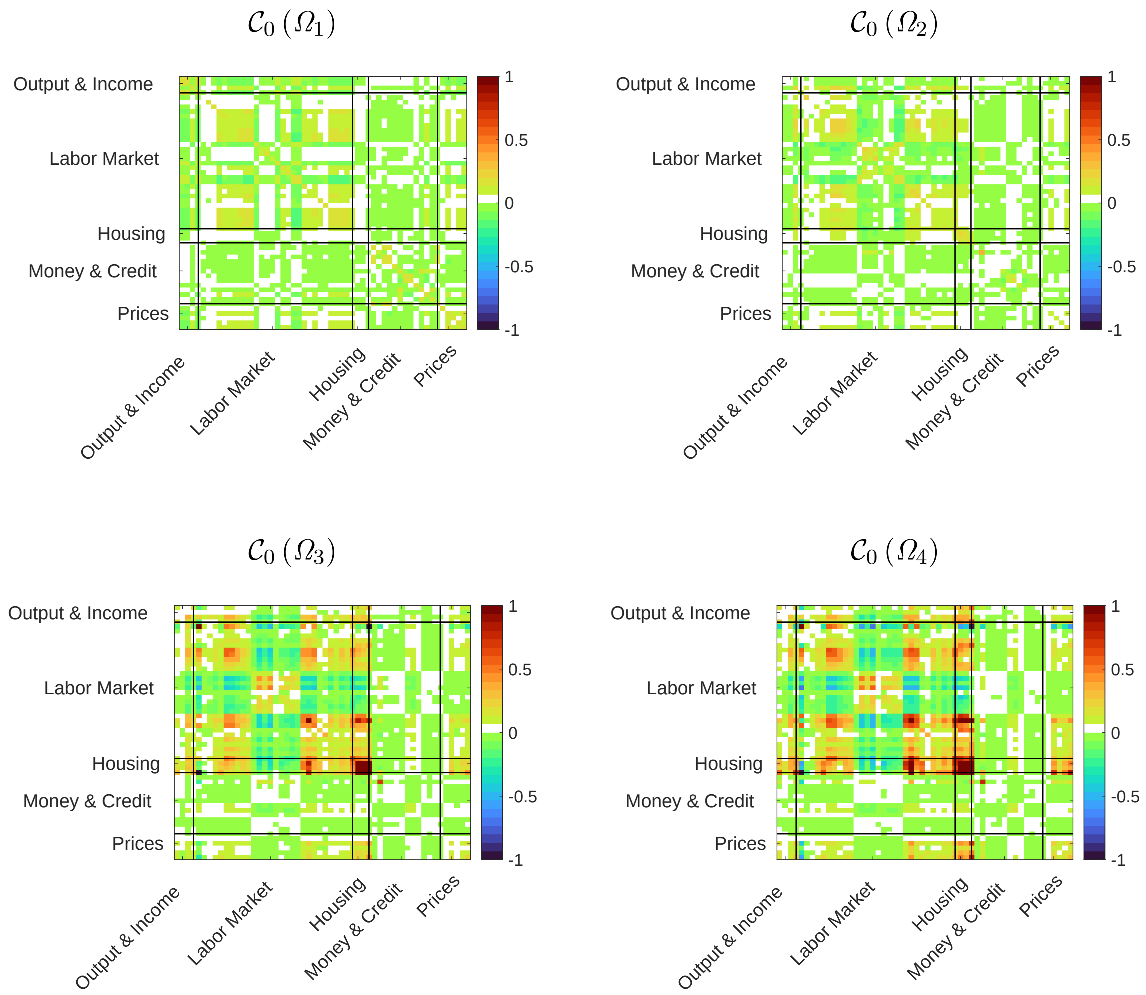

Figure 1: ALFRED DATASET: COVARIANCE MATRIX DECOMPOSITION BY ITS CYCLICAL COMPONENTS

Notes: Cycle length are: up to 1 year (Ω_1); between 1 and 3 years (Ω_2); between 3 and 8 years (Ω_3); 8+ years (Ω_4). For the generic band $\Omega = [\underline{\omega}, \overline{\omega}]$, we consider the normalized band spectrum covariance $\mathcal{C}_0\left(\Omega\right) = 0.5\left(\overline{\omega} - \underline{\omega}\right)^{-1} \mathbf{C}_0\left(\Omega\right)$.

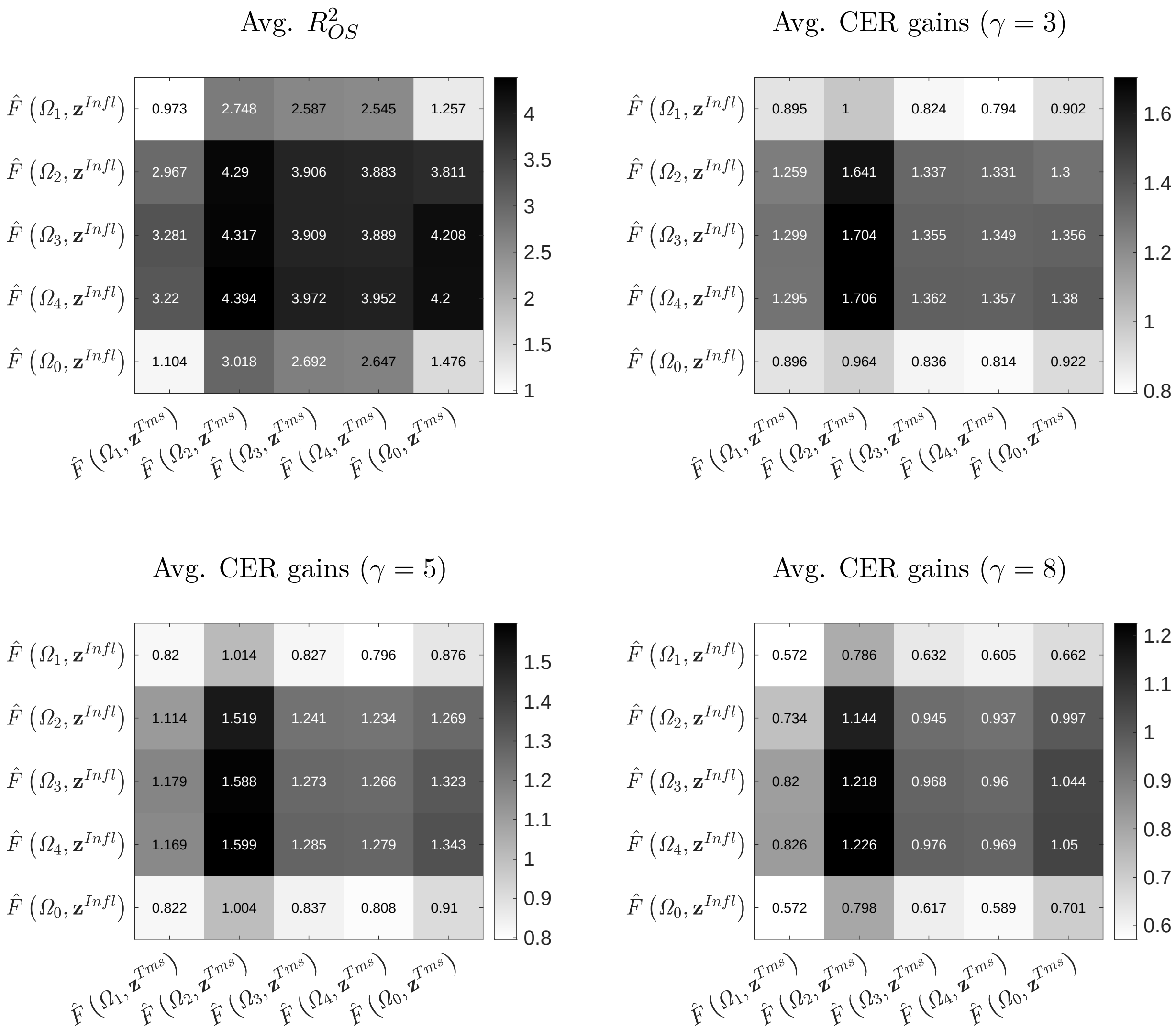

Avg. R^2_{OS}	$\hat{F}(\Omega_1, \mathbf{z}^{Tms})$	$\hat{F}(\Omega_2, \mathbf{z}^{Tms})$	$\hat{F}(\Omega_3, \mathbf{z}^{Tms})$	$\hat{F}(\Omega_4, \mathbf{z}^{Tms})$	$\hat{F}(\Omega_0, \mathbf{z}^{Tms})$
$\hat{F}(\Omega_1, \mathbf{z}^{Infl})$	0.973	2.748	2.587	2.545	1.257
$\hat{F}(\Omega_2, \mathbf{z}^{Infl})$	2.967	4.29	3.906	3.883	3.811
$\hat{F}(\Omega_3, \mathbf{z}^{Infl})$	3.281	4.317	3.909	3.889	4.208
$\hat{F}(\Omega_4, \mathbf{z}^{Infl})$	3.22	4.394	3.972	3.952	4.2
$\hat{F}(\Omega_0, \mathbf{z}^{Infl})$	1.104	3.018	2.692	2.647	1.476

Avg. CER gains ($\gamma = 3$)	$\hat{F}(\Omega_1, \mathbf{z}^{Tms})$	$\hat{F}(\Omega_2, \mathbf{z}^{Tms})$	$\hat{F}(\Omega_3, \mathbf{z}^{Tms})$	$\hat{F}(\Omega_4, \mathbf{z}^{Tms})$	$\hat{F}(\Omega_0, \mathbf{z}^{Tms})$
$\hat{F}(\Omega_1, \mathbf{z}^{Infl})$	0.895	1	0.824	0.794	0.902
$\hat{F}(\Omega_2, \mathbf{z}^{Infl})$	1.259	1.641	1.337	1.331	1.3
$\hat{F}(\Omega_3, \mathbf{z}^{Infl})$	1.299	1.704	1.355	1.349	1.356
$\hat{F}(\Omega_4, \mathbf{z}^{Infl})$	1.295	1.706	1.362	1.357	1.38
$\hat{F}(\Omega_0, \mathbf{z}^{Infl})$	0.896	0.964	0.836	0.814	0.922

Avg. CER gains ($\gamma = 5$)	$\hat{F}(\Omega_1, \mathbf{z}^{Tms})$	$\hat{F}(\Omega_2, \mathbf{z}^{Tms})$	$\hat{F}(\Omega_3, \mathbf{z}^{Tms})$	$\hat{F}(\Omega_4, \mathbf{z}^{Tms})$	$\hat{F}(\Omega_0, \mathbf{z}^{Tms})$
$\hat{F}(\Omega_1, \mathbf{z}^{Infl})$	0.82	1.014	0.827	0.796	0.876
$\hat{F}(\Omega_2, \mathbf{z}^{Infl})$	1.114	1.519	1.241	1.234	1.269
$\hat{F}(\Omega_3, \mathbf{z}^{Infl})$	1.179	1.588	1.273	1.266	1.323
$\hat{F}(\Omega_4, \mathbf{z}^{Infl})$	1.169	1.599	1.285	1.279	1.343
$\hat{F}(\Omega_0, \mathbf{z}^{Infl})$	0.822	1.004	0.837	0.808	0.91

Avg. CER gains ($\gamma = 8$)	$\hat{F}(\Omega_1, \mathbf{z}^{Tms})$	$\hat{F}(\Omega_2, \mathbf{z}^{Tms})$	$\hat{F}(\Omega_3, \mathbf{z}^{Tms})$	$\hat{F}(\Omega_4, \mathbf{z}^{Tms})$	$\hat{F}(\Omega_0, \mathbf{z}^{Tms})$
$\hat{F}(\Omega_1, \mathbf{z}^{Infl})$	0.572	0.786	0.632	0.605	0.662
$\hat{F}(\Omega_2, \mathbf{z}^{Infl})$	0.734	1.144	0.945	0.937	0.997
$\hat{F}(\Omega_3, \mathbf{z}^{Infl})$	0.82	1.218	0.968	0.96	1.044
$\hat{F}(\Omega_4, \mathbf{z}^{Infl})$	0.826	1.226	0.976	0.969	1.05
$\hat{F}(\Omega_0, \mathbf{z}^{Infl})$	0.572	0.798	0.617	0.589	0.701

Figure 2: Average R^2_{OS} and CER gains using all combinations of two predictors

Notes: Average out-of-sample R^2 and CER gains under mean-variance preferences across maturities corresponding to the predictions obtained as in equation (18) for any $i, j = 0, 1, \ldots, 4$.

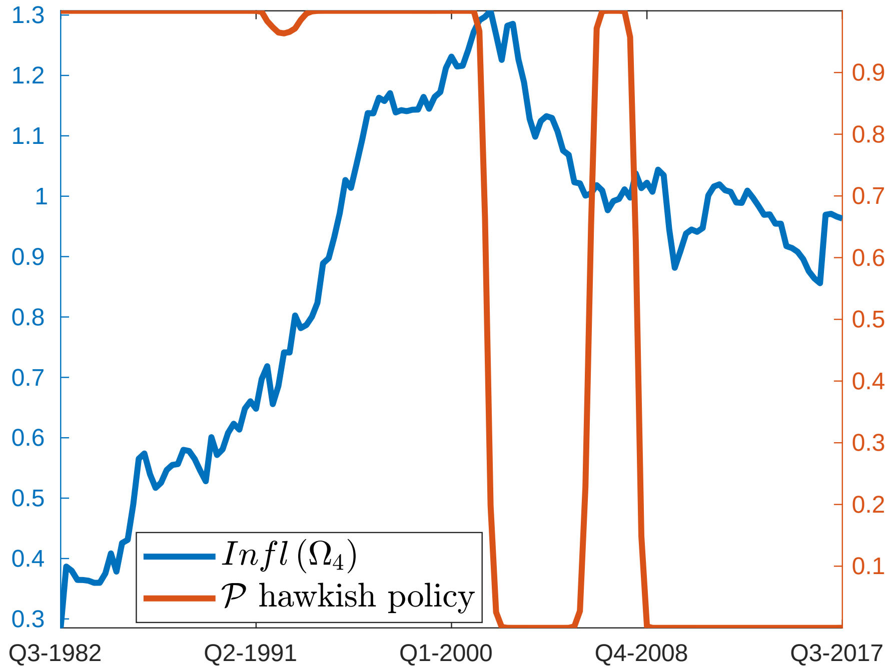

Figure 3: MONETARY POLICY STANCE AND INFLATION FACTOR'S UTILITY GAINS

Notes: The blue line are the cumulative quarterly utility gains with respect to the historical average benchmark associated with the predictions $Infl\,(\Omega_4)$, obtained as described in Section 4. The red line is the smoothed probability of hawkish monetary policy estimated by Bianchi et al. (2022).

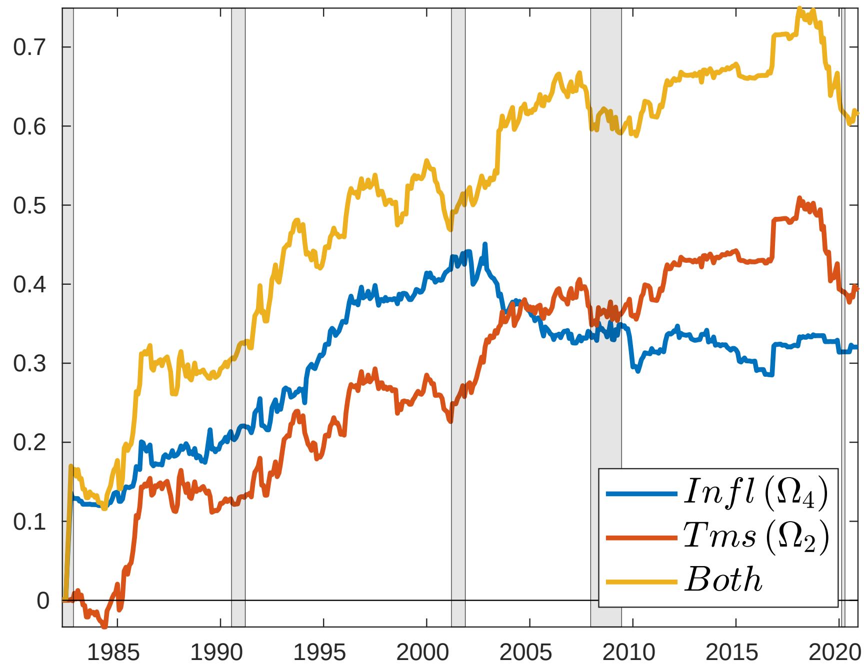

Figure 4: Cumulative utility gains

Notes: Baseline mean-variance exercise with $\gamma = 5$: cumulative monthly utility gains with respect to the historical average benchmark associated with the predictions $Infl\,(\Omega_4)$, $Tms\,(\Omega_2)$, $Both$ obtained as described in Section 4. Shaded areas denote NBER recessions.

Appendix

A. Frequency-specific factor estimation

A.1. Consistent estimation of the factor space

In this section we establish the consistent estimation of the space spanned by frequency-specific factors which motivates the use of estimated factors in our predictive regressions as if such factors were observed.

We begin with an unfeasible estimator $\widetilde{\mathbf{F}}(\Omega)$ of frequency-specific factors $\mathbf{F}(\Omega)$ based on a continuum of frequencies within the generic band $\Omega = [\underline{\omega}, \overline{\omega}]$ and show that its asymptotic properties are identical to the those of the principal estimator when latent factors are not frequency-specific. That is, the space spanned by the factors is estimated at the usual rate $\min(N, T)$.

Then, we cast a T-dimensional grid of Fourier frequencies ω_1, ω_2, $\ldots$, ω_T over $[-\pi, \pi]$ and estimate frequency-specific factors in the band Ω using the subset of frequencies ω_l, ω_{l+1}, $\ldots$, ω_u where l is the smallest integer such that $\underline{\omega} \leq \omega_l$ and u the largest integer such that $\omega_u \leq \overline{\omega}$ (to keep the notation simple we suppress the dependence of ω_u and ω_l on Ω). Being Ω an arbitrary fixed band, the number of available frequencies $u - l + 1$ grows linearly with T as the interval between neighbouring Fourier frequencies shrinks with T^{-1}. Hence, the cardinality $|\Omega_T| = u - l + 1$ is $O(T)$. The feasible estimator so obtained, which is the one proposed in the main text, is such that the factor estimates recover the span of frequency-specific factors at rate $\min(N, T/(M_T \log M_T))$, where M_T is the bandwidth for the lag window estimator (9).

Without loss of generality, in the rest of this section we refer to the two-band example introduced in Section 2.

For $j = 1, 2$, define the N-dimensional vectors $\mathbf{X}_t(\Omega_j) = \int_{\omega\in\Omega_j} \mathcal{X}_\omega e^{\iota\omega t} d\omega$ and $\mathbf{e}_t(\Omega_j) = \int_{\omega\in\Omega_j} \mathcal{E}_\omega e^{\iota\omega t} d\omega$, the $T \times N$ matrices $\mathbf{X}(\Omega_j) = (\mathbf{X}_1(\Omega_j), \mathbf{X}_2(\Omega_j), \cdots, \mathbf{X}_T(\Omega_j))'$ and $\mathbf{E}(\Omega_j) = (\mathbf{e}_1(\Omega_j), \mathbf{e}_2(\Omega_j), \cdots, \mathbf{e}_T(\Omega_j))'$ with generic entries $x_{it}(\Omega_j)$ and $e_{it}(\Omega_j)$, respectively, and the T-dimensional vectors $\mathbf{e}_i = (e_{i1}, e_{i2}, \cdots, e_{iT})'$, $\mathbf{e}_i(\Omega_j) = (e_{i1}(\Omega_j), e_{i2}(\Omega_j), \cdots, e_{iT}(\Omega_j))'$. We will use the singular value decomposition

$$
\begin{aligned}
(NT)^{-1/2}\mathbf{X}(\Omega_j) &= U_{NT}(\Omega_j) D_{NT}(\Omega_j) V_{NT}(\Omega_j)' \\
&= U_{NT,r}(\Omega_j) D_{NT,r}(\Omega_j) V_{NT,r}(\Omega_j)' + U_{NT,N-r}(\Omega_j) D_{NT,N-r}(\Omega_j) V_{NT,N-r}(\Omega_j)'
\end{aligned}
$$

where the diagonal entries of $D_{NT}(\Omega_j)$ are sorted in decreasing order. Finally, we use the Frobenius norm $\|A\| = \sqrt{tr(AA')}$.

Assumption 1. *For $i = 1, 2$*

(i) $E(e_{it}|\Lambda_1, \Lambda_2, \mathbf{F}_t(\Omega_1), \mathbf{F}_t(\Omega_2)) = 0$

(ii) It exists $M < \infty$ such that

(a) $E\left(N^{-1/2}\sum_{i=1}^{N}\left(e_{it}e_{is} - E\left(e_{it}e_{is}\right)\right)\right)^2 \leq M$;

(b) $T^{-1}\sum_{t=1}^{T}\sum_{s=1}^{T}\left|E\left(e_{it}e_{is}\right)\right| \leq M$, *for all* i;

(c) $N^{-1}T^{-1/2}\left\|\mathbf{e}_t'\mathbf{E}'\right\| = O_p\left(\min\left(N^{-1/2}, T^{-1/2}\right)\right)$, *for all* i;

(d) $T^{-1}N^{-1/2}\left\|\mathbf{e}_i'\mathbf{E}\right\| = O_p\left(\min\left(N^{-1/2}, T^{-1/2}\right)\right)$, *for all* t.

Assumption 2. *For* $j = 1, 2$

(i) $lim_{N\to\infty}\ N^{-1}\Lambda_j'\Lambda_j = \mathbf{C}_{\Lambda,j}$

(ii) $plim_{T\to\infty}\ T^{-1}\mathbf{F}\left(\Omega_j\right)'\mathbf{F}\left(\Omega_j\right) = \mathbf{C}_F\left(\Omega_j\right)$

where $\mathbf{C}_{\Lambda,j}$ *and* $\mathbf{C}_F\left(\Omega_j\right)$ *are positive definite with distinct eigenvalues.*

Assumption 3. *For* $j = 1, 2$

(i) $E\left\|N^{-1/2}\sum_i \Lambda_j e_{it}\left(\Omega_j\right)\right\|^2 \leq M$ *and* $(NT)^{-1}\mathbf{e}_t\left(\Omega_j\right)'\mathbf{E}\left(\Omega_j\right)'\mathbf{F}\left(\Omega_j\right)' = O_p\left(\min\left(N^{-1}, T^{-1}\right)\right)$, *for each* t;

(ii) $E\left\|T^{-1/2}\sum_{t=1}^{T}\mathbf{F}_t\left(\Omega_j\right)e_{it}\left(\Omega_j\right)\right\|^2 \leq M$ *and* $(NT)^{-1}\mathbf{e}_i\left(\Omega_j\right)'\mathbf{E}\left(\Omega_j\right)\Lambda_j = O_p\left(\min\left(N^{-1}, T^{-1}\right)\right)$, *for each* i.

Assumption 1 corresponds to Assumption A1 of Bai and Ng (2020), while Assumptions 2, 3 merely readapt their Assumptions A2, A3 to our context with frequency-specific factors. These assumptions ensure the existence of a factor structure. These three assumptions are enough to derive the properties of the unfeasible estimator.

Using the singular value decomposition of $(NT)^{-1/2}\mathbf{X}\left(\Omega_j\right)$ and the unfeasible factor estimator $\tilde{\mathbf{F}}\left(\Omega_j\right) = \sqrt{T}U_{NT,r}\left(\Omega_j\right)$ we have

$$(NT)^{-1}\mathbf{X}\left(\Omega_j\right)\mathbf{X}\left(\Omega_j\right)'\tilde{\mathbf{F}}\left(\Omega_j\right) = U_{NT}\left(\Omega_j\right)D_{NT}^2\left(\Omega_j\right)U_{NT}\left(\Omega_j\right)'\sqrt{T}U_{NT,r} = \tilde{\mathbf{F}}\left(\Omega_j\right)D_{NT,r}^2\left(\Omega_j\right) \tag{19}$$

Using the definition of $\mathbf{X}\left(\Omega_j\right)$ we have

$$\mathbf{X}\left(\Omega_j\right)\mathbf{X}\left(\Omega_j\right)' = \mathbf{F}\left(\Omega_j\right)\Lambda_j'\Lambda_j\mathbf{F}\left(\Omega_j\right)' + \mathbf{F}\left(\Omega_j\right)\Lambda_j'\mathbf{E}\left(\Omega_j\right)' + \mathbf{E}\left(\Omega_j\right)\Lambda_j\mathbf{F}\left(\Omega_j\right)' + \mathbf{E}\left(\Omega_j\right)\mathbf{E}\left(\Omega_j\right)' \tag{20}$$

(19) and (20) imply that

$$\tilde{\mathbf{F}}\left(\Omega_j\right)D_{NT,r}^2\left(\Omega_j\right) = \frac{\mathbf{F}\left(\Omega_j\right)\Lambda_j'\Lambda_j\mathbf{F}\left(\Omega_j\right)' + \mathbf{F}\left(\Omega_j\right)\Lambda_j'\mathbf{E}\left(\Omega_j\right)' + \mathbf{E}\left(\Omega_j\right)\Lambda_j\mathbf{F}\left(\Omega_j\right)' + \mathbf{E}\left(\Omega_j\right)\mathbf{E}\left(\Omega_j\right)'}{NT}\tilde{\mathbf{F}}\left(\Omega_j\right)$$

Defining the rotation matrix $\tilde{H}_{NT}\left(\Omega_j\right) = \left(\frac{\Lambda_j'\Lambda_j}{N}\right)\left(\frac{\mathbf{F}\left(\Omega_j\right)\tilde{\mathbf{F}}\left(\Omega_j\right)}{T}\right)D_{NT,r}^{-2}\left(\Omega_j\right)$, we have

$$\tilde{\mathbf{F}}\left(\Omega_j\right) = \mathbf{F}\left(\Omega_j\right)\tilde{H}_{NT}\left(\Omega_j\right) + \left(\mathbf{F}\left(\Omega_j\right)\Lambda_j'\mathbf{E}\left(\Omega_j\right)' + \mathbf{E}\left(\Omega_j\right)\Lambda_j\mathbf{F}\left(\Omega_j\right)' + \mathbf{E}\left(\Omega_j\right)\mathbf{E}\left(\Omega_j\right)'\right)\frac{\tilde{\mathbf{F}}\left(\Omega_j\right)}{NT}D_{NT,r}^{-2}\left(\Omega_j\right)$$

Rearranging and taking norms gives

$$
\begin{aligned}
T^{-1}\left\|\tilde{\mathbf{F}}\left(\Omega_j\right)-\mathbf{F}\left(\Omega_j\right)\tilde{H}_{NT}\left(\Omega_j\right)\right\|^2 \leq \frac{2}{T}\left\|\frac{\mathbf{E}\left(\Omega_j\right)\Lambda_j}{N}\right\|^2 \frac{\left\|\mathbf{F}\left(\Omega_j\right)\right\|^2}{T}\left\|\tilde{\mathbf{F}}\left(\Omega_j\right)\right\|^2 T^{-1}\left\|D_{NT,r}\left(\Omega_j\right)^{-2}\right\|^2+ \\
+\left\|\frac{\mathbf{E}\left(\Omega_j\right)\mathbf{E}\left(\Omega_j\right)'}{NT}\right\|^2\left\|\tilde{\mathbf{F}}\left(\Omega_j\right)\right\|^2 T^{-1}\left\|D_{NT,r}\left(\Omega_j\right)^{-2}\right\|^2 \\
=A+B
\end{aligned}
$$

A is $O_p\left(N^{-1}\right)$ because $T^{-1}\left\|\frac{\mathbf{E}(\Omega_j)\Lambda_j}{N}\right\|^2$ is $O_p\left(N^{-1}\right)$ by Assumption 3, $\left\|\mathbf{F}\left(\Omega_j\right)\right\|^2 T^{-1}$ is $O_p(1)$ by Assumption 2, $\left\|\tilde{\mathbf{F}}\left(\Omega_j\right)\right\|^2 T^{-1}=r$ because $\tilde{\mathbf{F}}\left(\Omega_j\right)=\sqrt{T}U_{NT,r}\left(\Omega_j\right)$ and the columns of $U_{NT,r}\left(\Omega_j\right)$ are unit-length, $\left\|D_{NT,r}\left(\Omega_j\right)^{-1}\right\|^2$ is $O_p(1)$. To see the latter result note that

$$
\begin{aligned}
\left\|D_{NT,r}^2\left(\Omega_j\right)\right\| \leq \left\|D_{NT}^2\left(\Omega_j\right)\right\| \leq \left\|\frac{X\left(\Omega_j\right)X\left(\Omega_j\right)'}{NT}\right\| \\
\leq \left\|\frac{\mathbf{F}\left(\Omega_j\right)\mathbf{F}\left(\Omega_j\right)'}{T}\right\|\left\|\frac{\Lambda_j\Lambda_j'}{N}\right\|+2\left\|\frac{\mathbf{F}\left(\Omega_j\right)\Lambda_j'\mathbf{E}\left(\Omega_j\right)'}{NT}\right\|+\left\|\frac{\mathbf{E}\left(\Omega_j\right)\mathbf{E}\left(\Omega_j\right)'}{NT}\right\|
\end{aligned}
$$

where the last two terms are asymptotically negligible as discussed above, and by Assumption 2 the first term converges in probability to $\left\|\mathbf{C}_F\left(\Omega_j\right)\right\|\left\|\mathbf{C}_{\Lambda,j}\right\|$.

B is $O_p\left(T^{-1}\right)$ because, under Assumption 1, $\left\|\frac{\mathbf{E}(\Omega_j)\mathbf{E}(\Omega_j)'}{NT}\right\|^2 \leq \left\|\frac{\mathbf{E}\mathbf{E}'}{NT}\right\|^2=O_p\left(\min\left(N^{-1},T^{-1}\right)\right)$ where the last equality is established by Lemma 1 of Bai and Ng (2020) under Assumption 1.

Finally, noting that

$$
\left\|\tilde{H}_{NT}\left(\Omega_j\right)\right\| \leq \left\|\frac{\Lambda_j'\Lambda_j}{N}\right\|\left\|\frac{\mathbf{F}\left(\Omega_j\right)'\mathbf{F}\left(\Omega_j\right)}{T}\right\|^{1/2}\left\|\frac{\tilde{\mathbf{F}}\left(\Omega_j\right)'\tilde{\mathbf{F}}\left(\Omega_j\right)}{T}\right\|^{1/2}\left\|D_{NT,r}^{-2}\left(\Omega_j\right)\right\|=O_p(1)
$$

we obtain the result

$$
T^{-1}\left\|\tilde{\mathbf{F}}\left(\Omega_j\right)-\mathbf{F}\left(\Omega_j\right)H_{NT}\left(\Omega_j\right)\right\|^2=O_p\left(\max(N^{-1},T^{-1})\right)
$$

For the feasible band spectrum principal component estimator we need to replace $\mathbf{X}\left(\Omega_j\right)$ and $\mathbf{E}\left(\Omega_j\right)$ with $\hat{\mathbf{X}}\left(\Omega_j\right)=\left(\hat{\mathbf{X}}_1\left(\Omega_j\right),\hat{\mathbf{X}}_2\left(\Omega_j\right),\ldots,\hat{\mathbf{X}}_T\left(\Omega_j\right)\right)'$ and $\hat{\mathbf{E}}\left(\Omega_j\right)=\left(\hat{\mathbf{E}}_1\left(\Omega_j\right),\hat{\mathbf{E}}_2\left(\Omega_j\right),\ldots,\hat{\mathbf{E}}_T\left(\Omega_j\right)\right)'$, where $\hat{\mathbf{X}}_t(\Omega)=\sum_{\omega=\omega_l}^{\omega_u}\sum_{\lambda=\omega_1}^{\omega_T}\sqrt{g(\omega-\lambda)}\mathcal{X}_\lambda e^{\iota\lambda t}$, $\hat{\mathbf{E}}_t(\Omega)=\sum_{\omega=\omega_l}^{\omega_u}\sum_{\lambda=\omega_1}^{\omega_T}\sqrt{g(\omega-\lambda)}\mathcal{E}_\lambda e^{\iota\lambda t}$ and $g(\omega-\lambda)\equiv T^{-1}\sum_{j=-M_T}^{M_T}e^{-\iota(\omega-\lambda)j}K_j\left(M_T\right)$, and use the singular value decomposition

$$
(NT)^{-1/2}\hat{\mathbf{X}}\left(\Omega_j\right)=\hat{U}_{NT,r}\left(\Omega_j\right)\hat{D}_{NT,r}\left(\Omega_j\right)\hat{V}_{NT,r}\left(\Omega_j\right)'+\hat{U}_{NT,N-r}\left(\Omega_j\right)\hat{D}_{NT,N-r}\left(\Omega_j\right)\hat{V}_{NT,N-r}\left(\Omega_j\right)'
$$

The asymptotic properties of the estimator depend on those of the band spectrum covariance estimator (10). To derive these properties we introduce the following assumptions.

Assumption 4. $\mathbf{F}_t=\mathbf{N}(L)\mathbf{u}_t$ *where* $\mathbf{u}_t$ *is a* q*-dimensional zero-mean stochastic process with* $q\leq r<N$, *and* $\mathbf{N}(L)$ *is* $r\times q$*-dimensional and one-sided with absolutely summable coefficients.*

Assumption 5. *For $i \in \mathbb{N}$, $t \in \mathbb{Z}$*

$$e_{it} = \sum_{j=1}^{\infty}\sum_{k=0}^{\infty} \beta_{ij,k}\eta_{j,t-k}$$

and $(\mathbf{u}_t'\boldsymbol{\eta}_t')'$ is i.i.d. orthonormal, where $\boldsymbol{\eta}_t = (\eta_{1t}, \eta_{2t}, \dots)'$. Moreover, $\beta_{ij,k}$ is such that

$\sum_{j=1}^{\infty}\sum_{k=0}^{\infty} \beta_{ij,k}^2 < \infty$,

$|\beta_{is,k}| \leq B_{is}\rho^k$ *with* $\sum_{s=1}^{\infty} B_{is} \leq B$ *and* $\sum_{i=1}^{\infty} B_{is} \leq B$,

for some $0 < B_{is} < \infty$, $0 < B < \infty$ *and* $0 \leq \rho < 1$.

Assumption 6. *For $i \in \mathbb{N}$, $t \in \mathbb{Z}$, $j = 1, \dots, q$ there exist $p > 4$ and $0 < A < \infty$ such that $E(|u_{jt}|^p) \leq A$ and $E(|\eta_{it}|^p) \leq A$*

Assumption 7. *(i) The kernel function K is even, bounded, with support $[-1, 1]$ and such that*

1) for some $\kappa > 0$, $|K(u) - 1| = O(|u|^{\kappa})$ as $u \to 0$,

2) $\int_{-\infty}^{\infty} K^2(u)\, du < \infty$,

3) $\sum_{j\in\mathbb{Z}} sup_{|s-j|\leq 1} |K(jw) - K(sw)| = O(1)$, as $w \to 0$.

(ii) For some positive constants c_1, c_2, δ and $\underline{\delta}$ with $0 < \underline{\delta} < \delta < 1 < \underline{\delta}(2\kappa + 1)$, the bandwidth M_T is such that $c_1 T^{\underline{\delta}} \leq M_T \leq c_2 T^{\delta}$.

Assumptions 4 and 5 strengthen Assumption 3 since no weak correlation among factors and idiosyncratic terms is allowed for. This is a requirement for the estimation of the spectral density matrix, which is also typical in the generalized dynamic factor models originated from Forni et al. (2000). Assumptions 6 and 7 correspond to Assumptions 8 and 9 of Forni et al. (2017) and are needed to use the results on the upper bound for the variance of the spectral density estimator established by Wu and Zaffaroni (2018). Under these assumptions Forni et al. (2017) obtain the uniform convergence of the spectral density estimator, a result which in our context corresponds to Lemma 2.

Proposition 1. *Under Assumptions 2, 4, 5, 6, 7*

$$N^{-1}\left\|\hat{\mathbf{C}}_0(\Omega) - \mathbf{C}_0(\Omega)\right\| = O_p\left(\sqrt{\frac{M_T \log M_T}{T}}\right)$$

Using the singular value decomposition of $(NT)^{-1/2}\hat{\mathbf{X}}(\Omega_j)$ and the feasible factor estimator $\hat{\mathbf{F}}(\Omega_j) = \sqrt{T}\hat{U}_{NT,r}(\Omega_j)$ we have

$$\begin{aligned}
(NT)^{-1}\mathbf{X}(\Omega_j)\mathbf{X}(\Omega_j)'\hat{\mathbf{F}}(\Omega_j) &= (NT)^{-1}\left(\hat{\mathbf{X}}(\Omega_j)\hat{\mathbf{X}}(\Omega_j)'\hat{\mathbf{F}}(\Omega_j) + \mathbf{B}\hat{\mathbf{F}}(\Omega_j)\right) \\
&= \hat{U}_{NT}(\Omega_j)\hat{D}_{NT}^2(\Omega_j)\hat{U}_{NT}(\Omega_j)'\sqrt{T}\hat{U}_{NT,r} + (NT)^{-1}\mathbf{B}\hat{\mathbf{F}}(\Omega_j) \\
&= \hat{\mathbf{F}}(\Omega_j)\hat{D}_{NT,r}^2(\Omega_j) + (NT)^{-1}\mathbf{B}\hat{\mathbf{F}}(\Omega_j) \qquad (21)
\end{aligned}$$

where $\mathbf{B} \equiv \mathbf{X}(\Omega_j)\mathbf{X}(\Omega_j)' - \hat{\mathbf{X}}(\Omega_j)\hat{\mathbf{X}}(\Omega_j)'$. (21) and (20) imply

$$\hat{\mathbf{F}}(\Omega_j) = \mathbf{F}(\Omega_j)\hat{H}_{NT}(\Omega_j) + \Big(\mathbf{F}(\Omega_j)\Lambda_j'\mathbf{E}(\Omega_j)' + \mathbf{E}(\Omega_j)\Lambda_j\mathbf{F}(\Omega_j)' + \mathbf{E}(\Omega_j)\mathbf{E}(\Omega_j)' + \mathbf{B}\Big)\frac{\hat{\mathbf{F}}(\Omega_j)}{NT}\hat{D}_{NT,r}^{-2}(\Omega_j)$$

where $\hat{H}_{NT}(\Omega_j) \equiv \left(\frac{\Lambda_j'\Lambda_j}{N}\right)\left(\frac{\mathbf{F}(\Omega_j)\hat{\mathbf{F}}(\Omega_j)}{T}\right)\hat{D}_{NT,r}^{-2}(\Omega_j)$. Rearranging and taking norms gives

$$\begin{aligned} T^{-1}\left\|\hat{\mathbf{F}}(\Omega_j) - \mathbf{F}(\Omega_j)\hat{H}_{NT}(\Omega_j)\right\|^2 \leq \frac{2}{T}\left\|\frac{\mathbf{E}(\Omega_j)\Lambda_j}{N}\right\|^2 \frac{\|\mathbf{F}(\Omega_j)\|^2}{T}\left\|\hat{\mathbf{F}}(\Omega_j)\right\|^2 T^{-1}\left\|\hat{D}_{NT,r}(\Omega_j)^{-2}\right\|^2 + \\ + \left\|\frac{\mathbf{E}(\Omega_j)\mathbf{E}(\Omega_j)'}{NT}\right\|^2\left\|\hat{\mathbf{F}}(\Omega_j)\right\|^2 T^{-1}\left\|\hat{D}_{NT,r}(\Omega_j)^{-2}\right\|^2 + \\ + \left\|\frac{\mathbf{B}}{NT}\right\|^2\left\|\hat{\mathbf{F}}(\Omega_j)\right\|^2 T^{-1}\left\|\hat{D}_{NT,r}(\Omega_j)^{-2}\right\|^2 \end{aligned}$$

A similar argument as above for unfeasible estimator applies to the first two terms. For the last term note that $\left\|\frac{\mathbf{B}}{NT}\right\|^2 = \left\|\frac{\hat{\mathbf{C}}_0(\Omega) - \mathbf{C}_0(\Omega)}{N}\right\|^2 = O_p\left(T^{-1}M_T\log M_T\right)$ where the last equality is ensured by Proposition 1. To see this, note that

$$\begin{aligned} \hat{\mathbf{C}}_0(\Omega) = \sum_{\omega=\omega_l}^{\omega_u}\hat{\mathbf{S}}(\omega) &= \sum_{\omega}\sum_{|j|\leq M_T} e^{-\iota j\omega}K_j(M_T)\hat{\mathbf{C}}_j \\ &= \sum_{\omega}\sum_{|j|\leq M_T} e^{-\iota j\omega}K_j(M_T)T^{-1}\sum_{\lambda=\omega_1}^{\omega_T}\mathcal{X}_\lambda\mathcal{X}_\lambda' e^{\iota\lambda j} \\ &= \sum_{\omega}\sum_{\lambda}T^{-1}\sum_{|j|\leq M_T}K_j(M_T)e^{-\iota(\omega-\lambda)j}\mathcal{X}_\lambda\mathcal{X}_\lambda' \\ &= \sum_{\omega}\sum_{\lambda}g(\omega-\lambda)\mathcal{X}_\lambda\mathcal{X}_\lambda' = \hat{\mathbf{X}}(\Omega)'\hat{\mathbf{X}}(\Omega) \end{aligned}$$

where the second line exploits

$$\mathcal{X}_\lambda\mathcal{X}_\lambda' = \left(\frac{1}{\sqrt{T}}\sum_{t=1}^{T}\mathbf{X}_t e^{-\iota\lambda t}\right)\left(\frac{1}{\sqrt{T}}\sum_{j=1}^{T}\mathbf{X}_j e^{-\iota\lambda j}\right)' = \frac{1}{T}\sum_t\sum_j\mathbf{X}_t\mathbf{X}_j' e^{-\iota\lambda(t-j)} = \sum_{|k|\leq T-1}e^{-\iota\lambda k}\frac{1}{T}\sum_{t=|k|+1}^{T}\mathbf{X}_t\mathbf{X}_{t-|k|}'$$

(with $k \equiv t-j$) and the corresponding inverse Fourier transform for $\hat{\mathbf{C}}_j$.

Thanks to Assumption 7, it is straightforward to show that, similarly to $D_{NT,r}(\Omega_j)$ and $\tilde{H}_{NT}(\Omega_j)$, $\hat{D}_{NT,r}(\Omega_j)$ and $\hat{H}_{NT}(\Omega_j)$ are $O_p(1)$. As a result we have that

$$T^{-1}\left\|\hat{\mathbf{F}}(\Omega_j) - \mathbf{F}(\Omega_j)\hat{H}_{NT}(\Omega_j)\right\|^2 = O_p\left(\max\left(N^{-1}, T^{-1}M_T\log M_T\right)\right)$$

Proof of Proposition 1

$$N^{-1}\left\|\hat{\mathbf{C}}_0(\Omega)-\mathbf{C}_0(\Omega)\right\|=N^{-1}\left\|\frac{\pi}{|\Omega_T|}\sum_{\omega_k\in\Omega}\hat{\mathbf{S}}(\omega_k)-\int_\Omega\mathbf{S}(\omega)\,d\omega\right\|\leq$$
$$\leq N^{-1}\left\|\frac{\pi}{|\Omega_T|}\sum_{\omega_k\in\Omega}\left(\hat{\mathbf{S}}(\omega_k)-\mathbf{S}(\omega_k)\right)\right\|+N^{-1}\left\|\frac{\pi}{|\Omega_T|}\sum_{\omega_k\in\Omega}\mathbf{S}(\omega_k)-\int_\Omega\mathbf{S}(\omega)\,d\omega\right\|$$
$$=a+b$$

For a it holds that

$$\mathrm{E}\left(N^{-2}\sum_{i,j=1}^{N}\left|\frac{\pi}{|\Omega_T|}\sum_{\omega_k\in\Omega}\left(\hat{s}_{ij}(\omega_k)-s_{ij}(\omega_k)\right)\right|^2\right)\leq\mathrm{E}\left(N^{-2}\sum_{i,j=1}^{N}\pi\max_{\omega_k\in\Omega}\left|\hat{s}_{ij}(\omega_k)-s_{ij}(\omega_k)\right|^2\right)$$

By Lemma 2, the latter term is $O_p\left(T^{-1}M_T\log M_T\right)$, hence a is $O_p\left(T^{-1/2}\sqrt{M_T\log M_T}\right)$.

For b,

$$N^{-2}\sum_{i,j=1}^{N}\left|\frac{\pi}{|\Omega_T|}\sum_{\omega_k\in\Omega}s_{ij}(\omega_k)-\int_\Omega s_{ij}(\omega)\,d\omega\right|^2\leq N^{-2}\sum_{i,j=1}^{N}\frac{\pi}{|\Omega_T|}\sum_{\omega_k\in\Omega}\max_{\omega_{k-1}\leq\omega\leq\omega_k}\left|s_{ij}(\omega_k)-s_{ij}(\omega)\right|^2$$

Using Lemma 1 and noting that $|\Omega_T|$ is $O_p(T)$, the latter term is $O_p\left(T^{-1}\right)$, hence b is $O_p\left(T^{-1/2}\right)$.

□

Lemmata

Lemma 1. *Under Assumptions 2, 4, 5, $s_{ij}(\omega)$ possess derivatives of any order and are of bounded variation uniformly in $i,j\in\mathbb{N}$.*

Proof. Under Assumption 4, 5, $s_{ij}(\omega)=\lambda_{i1}\mathbf{S}_{F,1}(\omega)\lambda'_{j1}+\lambda_{i2}\mathbf{S}_{F,2}(\omega)\lambda'_{j2}+s^e_{ij}(\omega)$. Forni et al. (2017, Proposition 2) prove that under Assumption 5 the third term $s^e_{ij}(\omega)$ has derivatives of all orders and bounded variation uniformly in i, j. The first two terms are such that

$$\lambda_{i1}\mathbf{S}_{F,1}(\omega)\lambda'_{j1}+\lambda_{i2}\mathbf{S}_{F,2}(\omega)\lambda'_{j2}=\begin{cases}\lambda_{i1}\mathbf{S}_F(\omega)\lambda'_{j1} & \omega\in\Omega_1\\ \lambda_{i2}\mathbf{S}_F(\omega)\lambda'_{j2} & \omega\in\Omega_2\end{cases}$$

Say, without loss of generality, that $\omega\in\Omega_1$. By Assumption 4 (absolute summability) $\mathbf{C}_{F,k}=\mathrm{E}\left(\mathbf{F}_t\mathbf{F}'_{t-k}\right)=\sum_{j=0}^{\infty}N_{k+j}N'_j<\infty$, hence $\lambda_{i1}\mathbf{S}_F(\omega)\lambda'_{j1}=(2\pi)^{-1}\lambda_{i1}\sum_{k=-\infty}^{\infty}e^{-\iota k\omega}\mathbf{C}_{F,k}\lambda'_{j1}$ has derivatives of any order and is of bounded variation. □

Lemma 2. *Under Assumptions 2, 4, 5, 6, 7, for all T, and $i,j\in\mathbb{N}$ it exists a positive constant C such that*

$$E\left(\max_{\omega_k\in\Omega}\left|\hat{s}_{ij}(\omega_k)-s_{ij}(\omega_k)\right|^2\right)\leq CT^{-1}M_T\log M_T \tag{22}$$

Proof. The proof is trivial since

$$\mathrm{E}\left(\max_{\omega_k\in\Omega}\left|\hat{s}_{ij}\left(\omega_k\right)-s_{ij}\left(\omega_k\right)\right|^2\right)\leq \mathrm{E}\left(\max_{|k|\leq M_T}\left|\hat{s}_{ij}\left(\omega_k\right)-s_{ij}\left(\omega_k\right)\right|^2\right)\leq CT^{-1}M_T\log M_T$$

where the last inequality is established by Forni et al. (2017, Proposition 6). □

A.2. Simulation results

We generate $r=2$ common factors $\mathbf{F}_t=A\mathbf{F}_{t-1}+\eta_t$ with $A=diag\,(0.4,0.4)$, and idiosyncratic errors $e_{it}=0.8\varepsilon_{it}+0.2\epsilon_t$ where η_t, ε_{it} and ϵ_t are mutually independent *iid* $\mathrm{N}(0,1)$. So we have autocorrelated factors and weakly cross-sectional dependent errors. A $T\times N$ panel $\mathbf{X}$ is generated as described in equation (4) with $\Omega_2=[-\theta,\theta]$, and $\Omega_1=[-\pi,-\theta)\cup(\theta,\pi]$ considering three different scenarios.

DGP 1 : $\theta=\pi/2$, Λ_1, Λ_2 independently drawn from a uniform distribution in $[-1,1]$.

DGP 2 : $\theta=\pi/4$, Λ_1 and Λ_2 independently drawn from a uniform distribution in $[-1,1]$.

DGP 3 : $\theta=\pi/4$, $\Lambda_1=\Lambda_2$ drawn from a uniform distribution in $[-1,1]$.

We measure estimation accuracy by projecting estimated factors onto real ones and report trace-R^2 statistics

$$R^2\left(\hat{\mathbf{Y}},\mathbf{Y}\right)=tr\left(\hat{\mathbf{Y}}'P_Y\hat{\mathbf{Y}}\right)/tr\left(\hat{\mathbf{Y}}'\hat{\mathbf{Y}}\right) \tag{23}$$

of such multivariate projections, where $tr(\cdot)$ stands for trace, $P_Y=\mathbf{Y}\left(\mathbf{Y}'\mathbf{Y}\right)^{-1}\mathbf{Y}'$, $\mathbf{Y}$ and $\hat{\mathbf{Y}}$ are either $\mathbf{F}$, $\mathbf{F}\left(\Omega_1\right)$, $\mathbf{F}\left(\Omega_2\right)$ and $\hat{\mathbf{F}}$, $\hat{\mathbf{F}}\left(\Omega_1\right)$, $\hat{\mathbf{F}}\left(\Omega_2\right)$, respectively. The results for each DGP and $T\times N=[25\ 50\ 100\ 200]\times[25\ 50\ 100\ 200]$ are obtained as averages across 500 replications.

The trace-R^2 statistics in Table A.1 show that in presence of frequency-specific effects, that is under DGP 1 and DGP 2, the BSPC estimator yields mean-square consistent estimation of frequency-specific factors: as N and T grow $R^2\left(\hat{\mathbf{F}}\left(\Omega_1\right),\mathbf{F}\left(\Omega_1\right)\right)$ and $R^2\left(\hat{\mathbf{F}}\left(\Omega_2\right),\mathbf{F}\left(\Omega_2\right)\right)$ approach 1. On the contrary, under DGP 3, that is in absence of frequency-specific effects, the BSPC estimator estimates $\mathbf{F}_t$: $R^2\left(\hat{\mathbf{F}}\left(\Omega_1\right),\mathbf{F}\right)$ and $R^2\left(\hat{\mathbf{F}}\left(\Omega_2\right),\mathbf{F}\right)$ approach 1 while $R^2\left(\hat{\mathbf{F}}\left(\Omega_1\right),\mathbf{F}\left(\Omega_1\right)\right)$ and $R^2\left(\hat{\mathbf{F}}\left(\Omega_1\right),\mathbf{F}\left(\Omega_2\right)\right)$ do not. In fact, as discussed in Section 2.2.1, in this case the BSPC is a inefficient but consistent estimator of $\mathbf{F}$. Nonetheless, the loss of efficiency is very mild since the trace-R^2s of the two BSPC estimates, $R^2\left(\hat{\mathbf{F}}\left(\Omega_1\right),\mathbf{F}\right)$ and $R^2\left(\hat{\mathbf{F}}\left(\Omega_2\right),\mathbf{F}\right)$, are very close to those of the usual principal component estimator, $R^2\left(\hat{\mathbf{F}},\mathbf{F}\right)$.

The first two DGPs violate the usual assumptions for the consistent principal component estimation of $\mathbf{F}$ and, indeed, $\hat{\mathbf{F}}_t$ does not seem to converge to $\mathbf{F}_t$ (this is particularly evident for DGP 2). DGP 3 is instead a usual factor model and the good performance of $\hat{\mathbf{F}}$ is in line with well-known results in the factor model literature.

The finite-sample properties of the BSPC estimator under the first two DGPs are somehow inferior to those of the PC estimator under DGP 3, but still reasonable for sufficiently large N

and T. For example, in Figure A.1 we repeat the same exercise for $r = 1$ and $N = T = 200$ and find that true and estimated factors are nearly undistinguishable. The solid lines are the spectra obtained with the unfeasible lag-window estimator that uses true factors, the dashed lines are instead obtained using the factors estimated via BSPCs. In the first two DGPs the estimated spectra of $\hat{F}_t(\Omega_1)$ and $\hat{F}_t(\Omega_2)$ are very close to those obtained using the unfeasible estimator which observes $F_t(\Omega_1)$ and $F_t(\Omega_2)$. Under DGP 3 the estimated spectra of $\hat{F}_t(\Omega_1)$ and $\hat{F}_t(\Omega_2)$ are undistinguishable because $\hat{F}_t(\Omega_1)$ and $\hat{F}_t(\Omega_2)$ are both estimates of F_t (the confidence bands for $\hat{F}_t(\Omega_1)$ and $\hat{F}_t(\Omega_2)$ are also remarkably similar).

Table A.1: Simulation results.

	DGP 1				DGP 2				DGP 3			
	$R^2\left(\hat{\mathbf{F}}(\Omega_1), \mathbf{F}(\Omega_1)\right)$				$R^2\left(\hat{\mathbf{F}}(\Omega_1), \mathbf{F}(\Omega_1)\right)$				$R^2\left(\hat{\mathbf{F}}(\Omega_1), \mathbf{F}(\Omega_1)\right)$			
	$N = 25$	50	100	200	$N = 25$	50	100	200	$N = 25$	50	100	200
$T = 25$	0.543	0.677	0.751	0.818	0.728	0.826	0.878	0.918	0.531	0.552	0.566	0.568
50	0.583	0.733	0.826	0.902	0.774	0.870	0.929	0.962	0.491	0.506	0.513	0.523
100	0.625	0.762	0.863	0.927	0.797	0.886	0.940	0.969	0.485	0.507	0.521	0.520
200	0.643	0.773	0.875	0.932	0.813	0.893	0.946	0.972	0.491	0.507	0.517	0.520
	$R^2\left(\hat{\mathbf{F}}(\Omega_2), \mathbf{F}(\Omega_2)\right)$				$R^2\left(\hat{\mathbf{F}}(\Omega_2), \mathbf{F}(\Omega_2)\right)$				$R^2\left(\hat{\mathbf{F}}(\Omega_2), \mathbf{F}(\Omega_2)\right)$			
	$N = 25$	50	100	200	$N = 25$	50	100	200	$N = 25$	50	100	200
$T = 25$	0.781	0.836	0.865	0.884	0.607	0.682	0.715	0.761	0.426	0.446	0.449	0.459
50	0.837	0.888	0.919	0.929	0.720	0.804	0.851	0.883	0.454	0.473	0.483	0.485
100	0.861	0.910	0.940	0.956	0.763	0.845	0.895	0.928	0.454	0.465	0.467	0.479
200	0.874	0.926	0.957	0.969	0.782	0.866	0.922	0.947	0.445	0.462	0.468	0.475
	$R^2\left(\hat{\mathbf{F}}, \mathbf{F}\right)$				$R^2\left(\hat{\mathbf{F}}, \mathbf{F}\right)$				$R^2\left(\hat{\mathbf{F}}, \mathbf{F}\right)$			
	$N = 25$	50	100	200	$N = 25$	50	100	200	$N = 25$	50	100	200
$T = 25$	0.586	0.619	0.646	0.654	0.523	0.548	0.570	0.581	0.853	0.887	0.907	0.918
50	0.620	0.654	0.685	0.693	0.494	0.529	0.549	0.553	0.891	0.925	0.943	0.952
100	0.623	0.674	0.693	0.703	0.479	0.515	0.532	0.538	0.913	0.944	0.961	0.970
200	0.644	0.682	0.713	0.717	0.481	0.498	0.528	0.530	0.923	0.955	0.972	0.980
	$R^2\left(\hat{\mathbf{F}}(\Omega_1), \mathbf{F}\right)$				$R^2\left(\hat{\mathbf{F}}(\Omega_1), \mathbf{F}\right)$				$R^2\left(\hat{\mathbf{F}}(\Omega_1), \mathbf{F}\right)$			
	$N = 25$	50	100	200	$N = 25$	50	100	200	$N = 25$	50	100	200
$T = 25$	0.375	0.380	0.361	0.349	0.496	0.528	0.533	0.538	0.844	0.881	0.903	0.914
50	0.340	0.315	0.303	0.289	0.459	0.480	0.489	0.498	0.886	0.922	0.941	0.950
100	0.317	0.303	0.285	0.282	0.456	0.481	0.499	0.506	0.911	0.942	0.960	0.969
200	0.314	0.286	0.284	0.273	0.461	0.489	0.506	0.513	0.921	0.955	0.971	0.980
	$R^2\left(\hat{\mathbf{F}}(\Omega_2), \mathbf{F}\right)$				$R^2\left(\hat{\mathbf{F}}(\Omega_2), \mathbf{F}\right)$				$R^2\left(\hat{\mathbf{F}}(\Omega_2), \mathbf{F}\right)$			
	$N = 25$	50	100	200	$N = 25$	50	100	200	$N = 25$	50	100	200
$T = 25$	0.606	0.643	0.652	0.669	0.473	0.494	0.506	0.515	0.847	0.880	0.901	0.912
50	0.642	0.675	0.692	0.703	0.461	0.480	0.491	0.501	0.891	0.924	0.942	0.950
100	0.653	0.680	0.700	0.712	0.437	0.459	0.473	0.479	0.913	0.944	0.961	0.970
200	0.664	0.691	0.712	0.721	0.435	0.460	0.471	0.480	0.923	0.956	0.972	0.980

Notes: The table reports trace-R^2 statistics (23). Data generating processes and all details of the simulation exercise are described in Section A.2. T,N denote the dimension of the panel considered for each DGP.

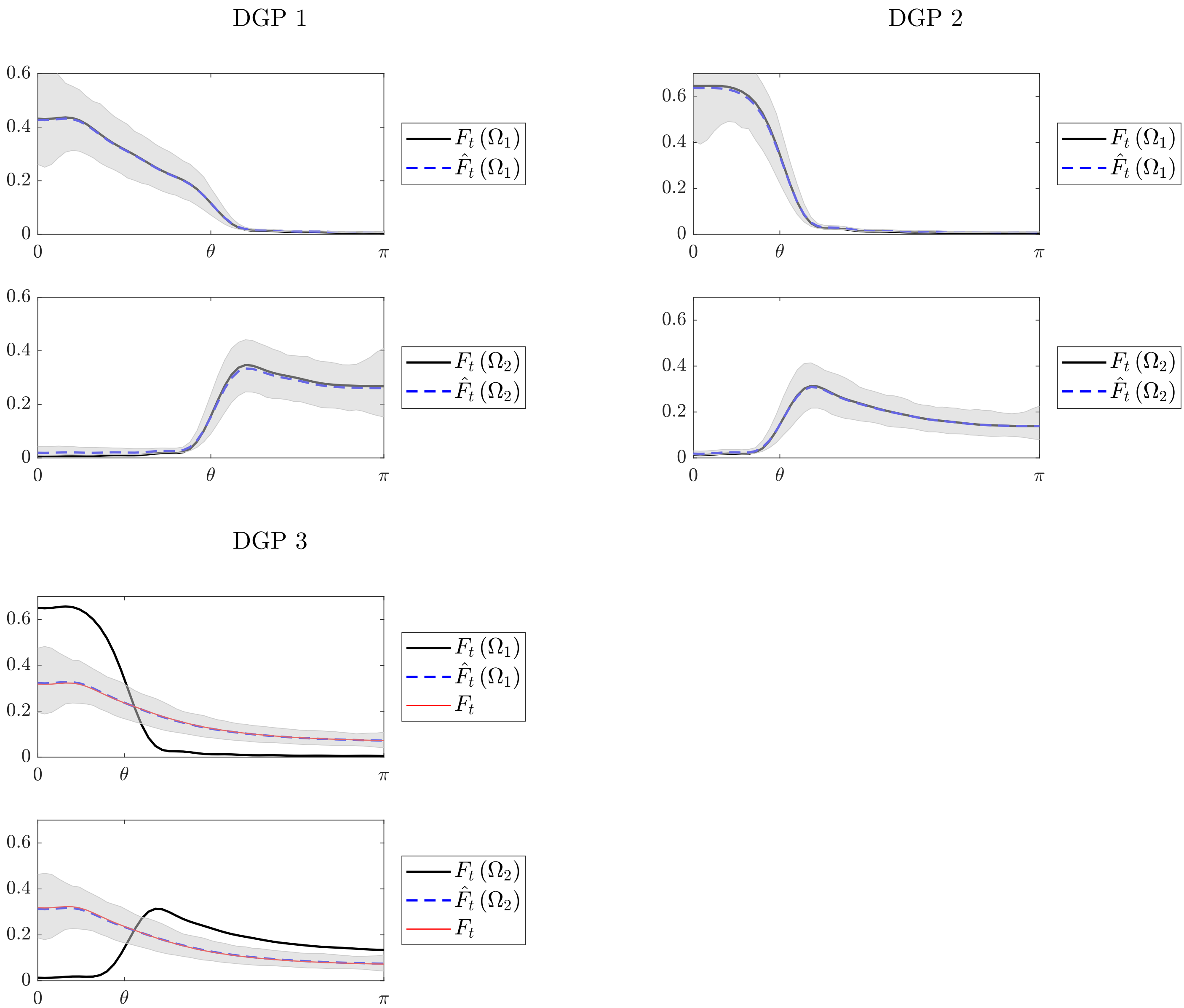

Figure A.1: SIMULATION: SPECTRAL DENSITY OF ESTIMATED FACTORS

Notes: Simulation exercise for the DGPs described in Section A.2 with $(T, N) = (200, 200)$ and $r = 1$. Spectral densities are estimated using a lag-window estimator (9). The solid lines are the spectra obtained with the unfeasible lag-window estimator that uses true factors, the dashed lines are instead obtained using the factors estimated via BSPCs. Shaded areas denote 95% confidence bands around the feasible BSPC estimates.

B. Real-time macroeconomic data

Table B.1: ALFRED data

	Mnemonic	Description	Tcode
1	AWHMAN	Avg Weekly Hours of Production and Nonsupervisory Employees: Manufacturing	1
2	AWHNONAG	Avg Weekly Hours Of Production And Nonsupervisory Employees: Total private	2
3	AWOTMAN	Avg Weekly Overtime Hours of Production and Nonsupervisory Employees: Manufacturing	2
4	CE16OV	Civilian Employment	5
5	CLF16OV	Civilian Labor Force	5
6	CPIAUCSL	Consumer Price Index for All Urban Consumers: All Items	6
7	CURRDD	Currency Component of M1 Plus Demand Deposits	6
8	CURRSL	Currency Component of M1	5
9	DEMDEPSL	Demand Deposits at Commercial Banks	6
10	DMANEMP	All Employees: Durable goods	5
11	DSPI	Disposable Personal Income	5
12	DSPIC96	Real Disposable Personal Income	5
13	HOUST	Housing Starts: Total: New Privately Owned Housing Units Started	4
14	HOUST1F	Privately Owned Housing Starts: 1-Unit Structures	4
15	HOUST2F	Housing Starts: 2-4 Units	4
16	INDPRO	Industrial Production Index	5
17	M1SL	M1 Money Stock	6
18	MANEMP	All Employees: Manufacturing	5
19	NDMANEMP	All Employees: Nondurable goods	5
20	OCDSL	Other Checkable Deposits	6
21	PAYEMS	All Employees: Total nonfarm	5
22	PCE	Personal Consumption Expenditures	5
23	PCEDG	Personal Consumption Expenditures: Durable Goods	5
24	PCEND	Personal Consumption Expenditures: Nondurable Goods	5
25	PCES	Personal Consumption Expenditures: Services	5
26	PI	Personal Income	5
27	SAVINGSL	Savings Deposits - Total	6
28	SRVPRD	All Employees: Service-Providing Industries	5
29	STDCBSL	Small Time Deposits at Commercial Banks	6
30	STDSL	Small Time Deposits - Total	6
31	STDTI	Small Time Deposits at Thrift Institutions	6
32	SVGCBSL	Savings Deposits at Commercial Banks	6
33	SVGTI	Savings Deposits at Thrift Institutions	6
34	SVSTCBSL	Savings and Small Time Deposits at Commercial Banks	6
35	TCDSL	Total Checkable Deposits	6
36	UEMP5TO14	Civilians Unemployed for 5-14 Weeks	5
37	UEMP15OV	Civilians Unemployed - 15 Weeks & Over	5
38	UEMP15T26	Civilians Unemployed for 15-26 Weeks	5
39	UEMP27OV	Civilians Unemployed for 27 Weeks and Over	5
40	UEMPLT5	Civilians Unemployed - Less Than 5 Weeks	5
41	UEMPMEAN	Average (Mean) Duration of Unemployment	2
42	UEMPMED	Median Duration of Unemployment	2
43	UNEMPLOY	Unemployed	5
44	UNRATE	Civilian Unemployment Rate	2
45	USCONS	All Employees: Construction	5
46	USFIRE	All Employees: Financial Activities	5
47	USGOOD	All Employees: Goods-Producing Industries	5
48	USGOVT	All Employees: Government	5
49	USMINE	All Employees: Mining and logging	5
50	USPRIV	All Employees: Total Private Industries	5
51	USSERV	All Employees: Other Services	5
52	USTPU	All Employees: Trade, Transportation & Utilities	5
53	USTRADE	All Employees: Retail Trade	5
54	USWTRADE	All Employees: Wholesale Trade	5

Notes: Tcode indicates the transformation adopted to achieve stationarity and is as follows. Letting $\tilde{x}_{it}$ be a raw variable and x_{it} its stationary transformation, we consider one of the following six transformation codes. 1: $x_{it} = \tilde{x}_{it}$; 2: $x_{it} = (1-L)\,\tilde{x}_{it}$; 3: $x_{it} = (1-L)^2\,\tilde{x}_{it}$; 4: $x_{it} = \ln(\tilde{x}_{it})$; 5: $x_{it} = (1-L)\ln\tilde{x}_{it}$; 6: $x_{it} = (1-L)^2\ln\tilde{x}_{it}$.

C. Additional empirical results

Table C.1: Out-of-sample R^2 using SUFF and sSUFF

	Maturities								
	2	3	4	5	6	7	8	9	10
SUFF	−6.899	−6.089	−5.515	−4.184	−5.078	−4.859	−5.419	−3.765	−5.110
sSUFF	−5.780	−5.276	−5.954	−5.220	−5.121	−5.165	−4.853	−3.593	−4.769
SUFF $(Infl)$	−3.848	−1.930	−1.121	−0.838	−0.393	−0.340	−0.703	−0.029	0.544**
sSUFF $(Infl)$	−7.865	−6.756	−7.163	−5.662	−5.526	−4.775	−4.734	−4.273	−5.010
SUFF (Tms)	−3.695	−2.732	−1.724	−3.037	−0.463	−0.878	−1.485	−3.437	−4.681
sSUFF (Tms)	−3.020	−0.943	−1.804	−1.261	−2.993	−8.760	−5.543	−4.936	−4.418
SUFF $(Infl, Tms)$	−6.158	−4.290	−4.965	−2.847	−2.294	0.166*	0.106*	−0.756	1.352**
sSUFF $(Infl, Tms)$	−3.255	−3.698	−3.709	−3.759	−4.434	−4.957	−5.629	−5.407	−5.514

Notes: SUFF and sSUFF are performed as described in Huang et al. (2023) and extracting 6 latent factors and 2 predictive indices. Where additional regressors are indicated in brackets the predictors are first projected onto the sieve space of such additional regressors as in Fan et al. (2017, 2021). *, **, *** denote statistical significance at 10, 5, 1 percent level using the test of Clark and West (2006) (only reported for positive R^2_{OS} values).

Table C.2: CER GAINS (POWER UTILITY)

	Maturities								
	2	3	4	5	6	7	8	9	10
					$\gamma = 3$				
$Infl\,(\Omega_1)$	0.126	0.166	0.261	0.201	0.061	−0.085	−0.132	−0.186	−0.260
$Infl\,(\Omega_2)$	0.387*	0.640*	0.804**	0.876**	0.892*	0.983*	1.174*	1.400**	1.571**
$Infl\,(\Omega_3)$	0.454*	0.709**	0.883**	0.960**	0.994*	1.076*	1.267*	1.511**	1.709**
$Infl\,(\Omega_4)$	0.449*	0.706**	0.881**	0.948**	0.991*	1.082*	1.273*	1.511**	1.700**
$Infl\,(\Omega_0)$	0.029	0.073	0.213	0.088	−0.034	−0.192	−0.228	−0.331	−0.410
$Tms\,(\Omega_1)$	0.395*	0.551*	0.498*	0.536	0.712	0.744	0.763	0.921	0.938
$Tms\,(\Omega_2)$	0.209	0.463*	0.725*	0.658	0.775	0.950	1.145*	1.647**	1.810**
$Tms\,(\Omega_3)$	0.139	0.287	0.415	0.386	0.542	0.879	1.133	1.580**	1.683**
$Tms\,(\Omega_4)$	0.129	0.271	0.414	0.378	0.525	0.862	1.109	1.552*	1.651*
$Tms\,(\Omega_0)$	0.437*	0.554*	0.490*	0.512	0.676	0.823	0.923	1.266**	1.277*
Both	0.440*	0.670*	0.990**	1.167**	1.543**	1.924**	2.308**	2.713**	2.965***
					$\gamma = 5$				
$Infl\,(\Omega_1)$	0.116	0.167	0.092	−0.050	−0.291	−0.310	−0.456	−0.612	−0.689
$Infl\,(\Omega_2)$	0.404*	0.646**	0.679**	0.683*	0.729*	0.943*	1.059*	0.907*	0.876
$Infl\,(\Omega_3)$	0.459**	0.712**	0.737**	0.750**	0.822*	1.040**	1.192**	1.031*	0.989*
$Infl\,(\Omega_4)$	0.460**	0.710**	0.732**	0.758**	0.823*	1.056**	1.213**	1.053*	1.013*
$Infl\,(\Omega_0)$	0.072	0.116	0.002	−0.141	−0.416	−0.455	−0.617	−0.781	−0.770
$Tms\,(\Omega_1)$	0.417*	0.497*	0.484*	0.675*	0.687*	0.822*	0.797	0.731	0.702
$Tms\,(\Omega_2)$	0.259	0.467*	0.490	0.642*	0.858*	1.361**	1.540**	1.713**	1.766**
$Tms\,(\Omega_3)$	0.153	0.228	0.246	0.461	0.659	1.103*	1.262*	1.537*	1.663*
$Tms\,(\Omega_4)$	0.144	0.221	0.239	0.452	0.645	1.067*	1.231*	1.518*	1.641*
$Tms\,(\Omega_0)$	0.429**	0.509**	0.446	0.660*	0.850*	1.055**	1.100**	1.068*	1.045
Both	0.437*	0.629*	0.900**	1.187**	1.569**	2.142***	2.356***	2.448***	2.596***
					$\gamma = 8$				
$Infl\,(\Omega_1)$	0.085	0.074	−0.050	−0.213	−0.451	−0.607	−0.666	−0.594	−0.632
$Infl\,(\Omega_2)$	0.394**	0.538**	0.462*	0.585**	0.722*	0.559	0.474	0.399	0.420
$Infl\,(\Omega_3)$	0.451**	0.592**	0.538*	0.681**	0.840**	0.662	0.574	0.472	0.466
$Infl\,(\Omega_4)$	0.452**	0.591**	0.548**	0.695**	0.860**	0.683	0.593	0.487	0.469
$Infl\,(\Omega_0)$	0.066	0.002	−0.150	−0.340	−0.570	−0.693	−0.788	−0.711	−0.713
$Tms\,(\Omega_1)$	0.359**	0.415*	0.507*	0.612**	0.704*	0.578	0.470	0.324	0.242
$Tms\,(\Omega_2)$	0.249*	0.299	0.494*	0.847**	1.168**	1.214**	1.146*	0.964	0.766
$Tms\,(\Omega_3)$	0.129	0.098	0.303	0.600*	0.857*	1.052*	1.062*	1.018	0.824
$Tms\,(\Omega_4)$	0.122	0.088	0.296	0.583	0.838*	1.020*	1.034	0.998	0.804
$Tms\,(\Omega_0)$	0.368**	0.423*	0.559**	0.729**	0.890**	0.776*	0.698	0.558	0.438
Both	0.420*	0.603**	0.855**	1.168**	1.553***	1.719**	1.702**	1.554**	1.487*

Notes: $\Omega_1 = [2\pi/12, \pi]$, $\Omega_2 = [2\pi/36, 2\pi/12]$, $\Omega_3 = [2\pi/96, 2\pi/36]$, $\Omega_4 = [0, 2\pi/96]$, $\Omega_0 = [0, \pi]$. *Both* forecasts are obtained as in equation (18) for $i = 4$ and $j = 2$. *, **, *** denote statistical significance at 10, 5, 1 percent level using the test of Diebold and Mariano (1995) (only reported for positive CER gains).

Table C.3: Sharpe ratios in expansions and recessions

	Maturities								
	2	3	4	5	6	7	8	9	10
	Expansions								
$Infl\,(\Omega_4)$	0.227	0.218	0.189	0.172	0.166	0.153	0.151	0.127	0.122
$Tms\,(\Omega_2)$	0.221	0.212	0.190	0.184	0.185	0.182	0.181	0.170	0.170
Both	0.214	0.202	0.196	0.193	0.196	0.191	0.192	0.184	0.186
	Recessions								
$Infl\,(\Omega_4)$	0.684	0.652	0.574	0.521	0.499	0.428	0.385	0.334	0.315
$Tms\,(\Omega_2)$	0.621	0.581	0.470	0.408	0.388	0.332	0.285	0.240	0.208
Both	0.711	0.664	0.578	0.525	0.514	0.452	0.397	0.328	0.290

Notes: $\Omega_2 = [2\pi/36, 2\pi/12]$, $\Omega_4 = [0, 2\pi/96]$. *Both* forecasts are obtained as in equation (18) for $i = 4$ and $j = 2$. Sharpe ratios are calculated from portfolio returns obtained as in the economic evaluation exercise described in Section 4.2 under mean-variance preferences and with $\gamma = 5$.

We analyse the term premium, defined as the gap between an n-year yield $y_t^{(n)}$ and its expectation component $n^{-1}E_t\left(y_t^{(1)} + y_{t+1}^{(1)} + \cdots + y_{t+n-1}^{(1)}\right)$, which can be estimated as

$$tp_t^{(n)} = \frac{1}{n}\left(\hat{rx}_{t+12}^{(n)} + \hat{rx}_{t+24}^{(n-1)} + \cdots + \hat{rx}_{t+12(n-1)}^{(2)}\right)$$

where the hats stand for predictions at time t. While the EH implies a constant term premium, rational expectation models predict instead a countercyclical term premium. Adopting Ludvigson and Ng (2009)'s VAR procedure for multi-step ahead forecasts, we measure the cyclical properties of the term premium implied by our *Both* forecasts. Following Ludvigson and Ng (2009) h-year-ahead predictions are obtained using a monthly vector autoregressive model with 12 lags that includes as variables the excess bond returns and a set of predictors. In Figure C.1 we show the term premium estimated using all maturities considered so far, that is $n = 10$, excluding or including our factors (top to bottom) against IP y-o-y growth. Both estimated term premia are countercyclical but the countercyclicality obtained including our predictors is almost twice as large — i.e. the correlation between the estimated term premium and industrial production growth is -0.29 versus -0.17. These values are very similar to those of Bianchi et al. (2021). All correlation coefficients are 1% significant.

$$Corr\left(IP_t, tp_t^{(10)}\right) = -0.17$$

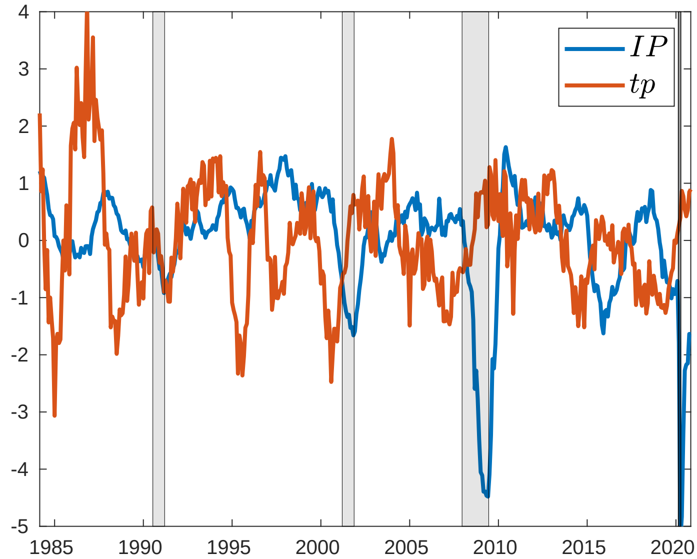

$$Corr\left(IP_t, tp_t^{(10)}\right) = -0.29$$

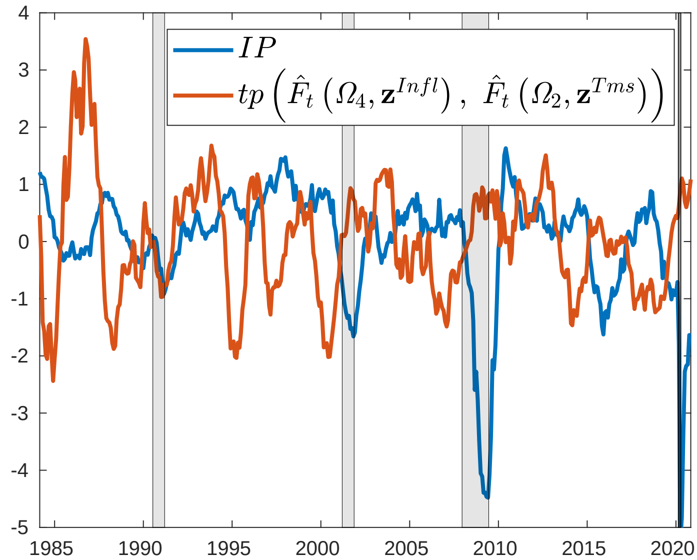

Figure C.1: Cyclical properties of the term premium

Notes: In the top plot, only yields are used to predict excess bond returns. In the bottom plot the expected excess bond returns are obtained using our macroeconomic predictors $\hat{F}_t\left(\Omega_4, \mathbf{z}^{Infl}\right)$ and $\hat{F}_t\left(\Omega_2, \mathbf{z}^{Tms}\right)$. Shaded areas denote NBER recessions.